NASA

Technical Memorandum 85054

STRUCTURE AND OTHER PROPERTIES OF JUPITER'S DISTANT MAGNETOTAIL

R.P. Lepping, M.D. Desch, L.W. Klein, E.C. Sittler, Jr., J.D. Sullivan, W.S. Kurth, and K.W. Behannon

JUNE 1983

National Aeronautics and Space Administration

Goddard Space Flight Center
Greenbelt, Maryland 20771

TM-85054
MIT-CSR-P-83-1

Structure and Other Properties of Jupiter's Distant Magnetotail

by

R. P. Lepping[1], M. D. Desch[1], L. W. Klein[2], E. C. Sittler, Jr.[1],
J. D. Sullivan[3], W. S. Kurth[4], and K. W. Behannon[1]

[1]Laboratory for Extraterrestrial Physics, Goddard Space Flight Center, Greenbelt, MD 20771

[2]Computer Sciences Corporation, 8728 Colesville Road, Silver Spring, MD 20910

[3]Plasma Fusion Center, Massachusetts Institute of Technology, Cambridge, MA 02139

[4]Department of Physics and Astronomy, The University of Iowa, Iowa City, IA 52242

June 1983

Submitted to the Journal of Geophysical Research

Abstract

Analyses using data from the Plasma Wave, Plasma Science, Planetary Radio Astronomy and Magnetometer experiments onboard Voyager 2 covering the period October 1980 to August 1981 are shown to provide compelling evidence for, and characteristics of, a Jovian magnetotail extending at least to 9,000 Jovian radii from the planet. Voyager 1 magnetic field and wave data from the same time period indicate that it was very unlikely that the distant Jovian tail was observed at that spacecraft. During approximately (25-day) periodic sightings of the tail by Voyager 2 the magnetic field tended to point radially towards or away from Jupiter, indicating preservation to large distances of the bipolar, lobe-like structure observed near the planet, as in the earth's case. This periodicity, along with various properties of the solar wind at this time, indicates that the tail is apparently influenced by recurrent solar wind features. Anomalous magnetic fields, not aligned with the nominal tail axis, also exist within the tail, especially in the low density, 'central' (core) region, indicating some complexity of internal structure. Approximately centered at each of the tail encounter periods we see broad-scale plasma velocity, density, and field magnitude decreases; the latter are not expected for a quasi-steady tail structure but probably indicate tail expansion to the position of the spacecraft. On a finer scale the field increases across the inbound boundary as expected for an outward pressure imbalance. We argue that a possible contributor to the internal pressure of the tail is a considerable amount of tailward flowing plasma, in addition to the expected internal field pressure. Magnetic field variance analyses provide quantitative evidence for field-line draping around the boundary of the tail and also show that internal tail-field transverse variations occur. We suggest that the Jovian tail has a quasi-periodically variable width (resembling a string of sausages) on a very long length scale, tens of thousands of Jupiter radii, due to the influence of the $\sim$ 25 day radial variation of the solar wind pressure. The tail is also apparently filamentary to some degree.

Introduction

Until the recent studies of the distant Jovian tail (Kurth et al., 1981, 1982b; Scarf et al., 1981, 1982, 1983; and Lepping et al., 1982) our knowledge of planetary magnetotails was restricted to the near-planet tail regions of Earth (Ness, 1965, 1969 and references therein; Behannon, 1968), Jupiter (Ness et al., 1979; Gurnett et al., 1980; Behannon et al., 1981; Goertz, 1981; and Schardt et al., 1981), Mercury (Siscoe et al., 1975), and the relatively distant tail regions of Earth (Villante, 1977 and references therein) at 500 and 1000 earth radii, and possibly at 3,000 earth radii (Intriligator et al., 1979). Scarf (1979) was the first to point out the possibility of the Voyager 2 spacecraft encountering the Jovian magnetotail while enroute to Saturn, and the further possibility of Saturn being in Jupiter's tail during the Voyager 2 Saturn encounter. Grzedzielski et al. (1981) have presented a model which predicts that the Jovian tail could be long enough (7-15 AU) and wide enough ($\sim$ 0.6 AU) to engulf Saturn's magnetosphere during the encounter. Evidence based on the spatial distribution of tail encounters (Lepping et al., 1982) suggests that the tail at times must be substantially wider than 0.6 AU, in fact, and we will argue below that it has a variable width, with its narrowest dimensions probably being $\lesssim$ 0.6 AU.

Kurth et. al. (1981, 1982b) and Lepping et. al. (1982) have presented criteria by which the distant Jovian tail events were initially identified in Voyager 2 wave, plasma, and magnetic field data. In particular, Plasma Wave Science (PWS) determines a tail event or candidate in terms of the presence of nonthermal continuum radiation (see Gurnett et al., 1979) and infers that the most certain tail encounter events are those whose estimated plasma densities are $< 4 \times 10^{-2}$ cm^{-3} (and most are below 10^{-2} cm^{-3}), based on the inferred electron plasma frequency. These are called "core" events, and the regions in which the density reaches these low values are the core regions; we shall use the same terminology. Plasma Science (PLS) identifications depend on the marked decrease of plasma density to values far below nominal solar wind values at the heliocentric distances of interest here, 7-9 AU. In Kurth et. al. (1982b), PWS and PLS data were used in combination to identify distant tail sightings (over 5-9 AU) adding considerable credence to the identifications, since neither the presence of nonthermal continuum radiation nor very

low density regions alone are sufficient indicators of a magnetotail. Both conditions can exist outside of the tail (see e.g., Kurth et. al., 1981).

In Lepping et. al. (1982), Voyager 2 Planetary Radio Astronomy (PRA) and Magnetometer (MAG) data were used in combination for distant Jovian tail identifications. As in the case of PWS, PRA tail identifications depend on the presence of (very low frequency, 1.2 kHz) nonthermal continuum radiation. MAG identifications depend on the high probability of tail lobe-like fields being present which, at the time and distance of the sightings, was demonstrated by near-alignment of the field with the Jupiter-spacecraft line. Although Jupiter-spacecraft aligned fields are not restricted to magnetotail regions, both the Parker spiral model and actual Interplanetary Magnetic Field (IMF) observations (Thomas and Smith, 1981), lead one to expect the IMF to have that alignment only infrequently at heliocentric distances of 7-9 AU.

The principal purposes (and approximate outline) of this paper are:

1. to provide a broad survey of the four data sets (PWS, PLS, PRA and MAG) from Voyager 2 over a period of $\sim$ 10 months downstream from Jupiter where an extended tail might be expected to be observed, in order to identify comprehensively the tail sightings and to determine gross characteristics;

2. to delineate the tail intervals as defined by MAG only, to complement PRA data and the work of Kurth et al. (1982b);

3. to show solar wind plasma and field magnitude variations during this period and relate the dynamics of the distant tail to them;

4. to provide a survey analysis of variations of the magnetic field, to further identify and characterize the tail events and their surrounding regions;

5. to analyse the field properties in the tail and its core statistically, and compare them to external (control) regions to help to define the structure and degree of complexity of the tail;

6. to quantify the discovered periodicity of tail sightings through auto- and cross-correlation analyses;

7. to study in detail the May 1981 event, which in most respects typifies the other prominent events, and to use it to examine the nature of the tail's boundary (is it a magnetopause as in the earth's case?);

8. to speculate on the large scale shape and dynamics of the tail on the basis of the apparent relation between tail dynamics and recurrent solar wind variations as demonstrated in (3);

9. to attempt to understand what entities play the major roles in balancing pressure across the tail boundary; and finally,

10. to provide arguments for the possibility that Saturn was in Jupiter's tail during the Voyager 2 Saturn encounter.

Before starting we take the point of view, guided by earlier work or justified by observations below, that: (A) the tail proper must contain magnetic field lines that appear directionally to connect back to Jupiter, (B) the outer boundary of the tail proper is a magnetopause current sheet, (C) within the tail a "core" region exists which, however, is not synonymous with the tail proper, i.e., it usually has a much smaller cross-section, (D) solar wind-like magnetosheath plasma exists outside the magnetopause, and (E) if wake plasma exists, it is probably external to the magnetopause. The reason for assuming statement (D) was discussed by Lepping et al. (1982). What had been described as "wake plasma" by Kurth et al. (1982b) we now believe was probably plasma internal to the tail and more characteristic of boundary layer plasma, somewhat similar to that of the earth's tail (Hones et al., 1972; Eastman, 1979; Sckopke and Paschmann, 1978).

Voyager 2 Trajectory

In Figure 1 two views of the Voyager 2 trajectory downstream from Jupiter for the period from October 1980 to August 1981 are shown. The top view represents the trajectory in cylindrical coordinates with cylindrical axis (X)

along the Sun-Jupiter line and shows distant Jovian tail encounters, denoted K, K, 1, 2, . . . 8, as identified and discussed by Lepping et. al. (1982) and Kurth et. al. (1982b) for this period. With the possible exceptions of events 7 and 8, all were core events, confined to a cone of half angle 12° as shown. The bottom view shows the trajectory in Jupiter's orbital plane (X-Y). The average aberrated tail position would differ from the X-axis by only 1.9° for a typical solar wind speed of 400 km/s at these distances from the sun.

Survey

Data from PWS, PLS, PRA and MAG experiments onboard Voyager 2 were examined for the period extending from Jupiter encounter to about a month beyond Saturn encounter. Figure 2 shows 287 days of data from three of these experiments, from day 310 (5 November) 1980 to day 230 (18 August) 1981, i.e., a period approximately centered around the expected point of closest approach to the nominal distant Jovian tail. The top panel displays 2-hour averaged wave amplitudes of continuum radiation centered at 1.2kHz, the lowest PRA frequency channel. The next panel shows daily averaged ion densities from PLS; the analysis as outlined in Kurth et al. (1982b) for the PLS data is used here. The bottom two panels are histograms of occurrence of particular magnetic field orientations. Specifically, the bottom panel shows vertical bars representing the percent of hours in a day for which the field had an angle of $\alpha > 150^{\circ}$, where α is the angle between the field and the direction to Jupiter with vertex at the spacecraft, as shown in Figure 3. Such fields, if in the Jovian tail, would be in the northern (N) lobe. Likewise, the second panel from the bottom gives the percent of hours in a day in which the field has either $\alpha > 150^{\circ}$ (N, for northern lobe) or $\alpha < 30^{\circ}$ (S, for southern lobe). Since α for the IMF is expected to have a value near 90° with high probability at these distances from the sun, the α-criterion is a relatively good one for discriminating between candidate tail fields and the IMF. The horizontal bars under the PRA panel labeled "TAIL" were, for events 1 through 8, determined by an examination of PRA and PWS (for significant nonthermal continuum radiation amplitudes) and PLS (for unusually low densities); events marked K and P are from Kurth et. al. (1982b). By design, none of the "TAIL" regions were identified by MAG criteria.

Table 1 lists the start and stop times for intervals 1 through 8. The 'CORE' events from Kurth et. al. (1982b) are based on inferred electron densities of $< 4 \times 10^{-2}$ cm^{-3} from the PWS continuum data and are usually well supported by correspondingly low PLS densities (see Table 2 of Kurth et. al., 1982b). The CONTROL sets shown at the top of the figure were chosen because of the absence of tail-like features at those times, again according to PWS, PRA, and PLS data only, and collectively they have about the same duration as the sum of the tail events 1 through 8. Table 2 lists the start and stop times for these CONTROL intervals, which we believe have characteristics of typical solar wind regions at this time. For example, PLS densities in the CONTROL regions were on average usually close to 10^{-1} cm^{-3}, as expected at this radial distance. The overall agreement among the four data sets with respect to affirming encounters with the distant Jovian tail is very good, especially for events 1 through 6. These data show that during "TAIL" regions: (1) continuum radiation is detected by one or both of the PWS (see Kurth et. al., 1982b) or PRA instruments, (2) density measured by PLS is either very low or relatively low with respect to neighboring regions, (3) lobe-like magnetic fields are present, and (4) CORE regions exist for most major events. Whether events 7 and 8 are CORE or even TAIL events is controversial, and arguments concerning their legitimacy are given in Kurth et al, (1982b). We retain them here as probable tail encounters, based mainly on the PLS and MAG data and to some degree on the wave data.

Two outstanding features of Figure 2 should be stressed. First the events appear to occur nearly periodically; Lepping et al. (1982) compute an average period of 26.5 days between events. This periodic behavior and its apparent cause will be discussed below. Second, the occurrence of 'toward' and 'away' tail fields (with respect to Jupiter) obeyed a distinct pattern. The bottom two panels of the figure indicate that Voyager 2 was observing northern lobe fields during the tail encounters almost exclusively until about day 130 of 1981 when a crossover to almost purely southern lobe fields occurred. The reason for this crossover is not clear and could be due to a combination of effects. For example, as shown in Kurth et al. (1982b, their Figure 3) the spacecraft never crosses the orbital plane of Jupiter and moves slowly with respect to that plane over the many months of interest here. So latitudinal change of the spacecraft in itself is not a likely candidate for

this crossover. Either a large twist or tilt of the tail about the X-axis (Figure 1) could explain it, since the closest approach point of the spacecraft to the expected average aberrated tail occurs only three weeks before day 130, i.e., within event 4, as the spacecraft travels 'westward'. However, Jupiter's rotational axis is tilted only $\sim 3^\circ$ with respect to its orbital plane, so this is not expected to cause a significant long term average tilt of the tail. Effects in the tail due to the tilt of the magnetic dipole of Jupiter would be expected to be periodic and not likely to cause a single occurrence. Other large scale twisting or tilting of the tail could arise from an as yet unexplained feature of the solar wind interaction with it.

Tail candidate events occurring between Voyager 2 Jupiter encounter and events K-K, shown at the beginning of Figure 2, are discussed by Kurth et. al. (1981, 1982b) and will not be discussed here; none of those earlier events, with the exception of the one near Jupiter (Kurth et. al., 1981), was a core event. It has recently been pointed out (F. L. Scarf, private communication) that Voyager 2 PWS and PLS data reveal the probable existence of two post-Saturn Jovian tail encounters; these are discussed in Scarf et. al. (1983).

From considerations of all four experiments, the most prominent events shown in Figure 2 are events 2 through 5. Event 2 has been discussed in detail by Scarf et. al. (1981) and Lepping et. al. (1982), and event 3 by Kurth et. al. (1982b). Event 4 will be discussed in a future paper. It appears to be most complex generally, was long lasting, was composed of fields of both lobes (mostly northern), and occurred near and around the average aberrated tail point (day 105). In another section of the present paper we shall discuss various features of (the May) event 5 which, in contrast to the earlier events, has intense continuum radiation and primarily southern lobe fields.

Solar Wind-Tail Interaction

As mentioned above, prominent signatures of the Jovian magnetotail were observed nearly periodically every $\sim$ 26 days. This quasi-regular reappearance during each 25-day solar rotation cycle must depend on the structural

characteristics of the solar wind between 5 and 10 AU and on the nature of the wind-tail interaction. Between the sun and a few AU the solar wind speed profile is dominated by the effects of discrete high-speed streams emitted from localized regions on the sun. Internal forces associated with the momentum flux of the streams and with related pressure gradients act to accelerate slow material and decelerate fast material (Burlaga, 1983a). The result is a narrowing of the solar wind bulk speed distribution at large distances from the sun, with the wind speed tending to approach the mean value at all solar longitudes near the equatorial plane (Collard et al., 1982).

This leveling or destruction of fast streams is accompanied by the development of large-scale pressure ridges or waves (Belcher et al., 1981; Burlaga, 1983a,b). Thus the solar wind is characterized more predominantly at these distances by alternating compressions and rarefactions as seen in the plasma density and magnetic field magnitude observations and less by velocity variations; the latter are found to be less pronounced and more irregular.

These characteristics are illustrated for the period of extended Jovian tail observations of interest here in the top 3 panels of Figure 4, which show, from the top, the speed V, field magnitude B and ion density N; note that speed determinations are not completely reliable for densities less than 10^{-2} cm^{-3}. At the bottom of the figure we include for comparison data indicating detection of the tail. The important features to note in Figure 4 are the lack of a clear, organized stream pattern at these distances (7-9 AU), whereas a pattern of correlated recurring magnetic field and density compression and rarefaction features is clearly in evidence. It is additionally obvious that the tail "events" had a strong tendency to occur during density minima, i.e., periods of rarefaction. As these also appear to have coincided with times of generally low to average wind speed, it is apparent that detection of the Jovian tail at Voyager 2 coincided with minima in the solar wind bulk flow pressure or "ram" pressure, ρV^2. This quantity is not plotted but should track the density, N, to a good approximation (see, for example, Figure 10). Also since B and N are strongly correlated, as shown in Figure 4, the solar wind magnetic field pressure $B^2/8\pi$ is correlated with N; this is generally the case for the distant solar wind (Burlaga, 1983a, b). Since the kinetic pressure of the solar wind is directly dependent on N also,

then the total pressure impinging on the tail boundary (i.e., a component of the ram pressure, the magnetic field pressure, and the kinetic pressure) will be strongly correlated with the almost periodically varing N, with an expected 25-day period.

Magnetic Field Variance Analysis

Lepping et al. (1982; see especially Figures 3 and 4 of that paper) suggested that draped magnetic field lines occurred immediately adjacent and external to the apparent boundary of Jupiter's tail for the February 1981 (no. 2) event. Field line draping around the earth's magnetopause is well known (Fairfield, 1967). In an attempt to look for such draping for all of the Jupiter distant-tail events, we performed a variance analysis of the field using data from day 310 of 1980 to 230 of 1981; a similar application of a variance analysis to Jupiter's magnetosheath fields was carried out by Lepping et al. (1981). It is appropriate to use such an analysis, because we are searching for indications of fields constrained to lie approximately parallel to a boundary surface, and hence we wish to determine the normal ($\hat{n}$) to that surface, i.e., the minimum variance direction. In particular, the variance analysis technique of Sonnerup and Cahill (1967) was applied to all hour averages of the magnetic field over this period for a series of overlapping 12-hour analysis intervals with the start hour progressively slipped by 3 hours for each calculated variance ellipsoid. The major axes of each ellipsoid were used for judging the quality and meaning of the estimated minimum variance direction.

Where $\alpha_{\hat{n}}$, a cone angle of a normal, is defined in the same manner as α was for the field itself, as shown in Figure 3, but now for the hemisphere toward the planet only ($0° \leq \alpha_{\hat{n}} \leq 90°$), it is reasonable to expect then that normals having $\alpha_{\hat{n}}$ at or near 90° are predominantly associated with tail encounters. By contrast, typical IMF variations at this distance from the sun (7-9 AU) are expected to have minimum variance normals that clustered at or near 0° and that avoid values near 90° because of the predominant orientation of the IMF in this region (Thomas and Smith, 1981). Appendix A gives the eigenvalue criteria and other conditions associated with restrictions on the variance computations. Almost all of the acceptable minimum variance normal

directions for the full 287-day period of interest were very close to being perpendicular to their local field directions, i.e., for each calculation both the field and its variations were almost always locally confined to a plane when the eigenvalue ratio criteria were satisfied. A percent distribution of all acceptable normals, IMF- and tail-associated, is shown in Figure 5 in terms of heliographic longitude ($\lambda_{\hat{n}}$) and latitude ($\delta_{\hat{n}}$) angles as well as in terms of $\alpha_{\hat{n}}$. Figure 5 clearly indicates that IMF associated normals dominate: $\lambda_{\hat{n}}$ peaks at 160° (i.e., near 180°), $\alpha_{\hat{n}}$ is broadly distributed and weighted somewhat disproportionately toward lower values, and 24% of the normals, i.e., 311 out of 1304 cases, lie above $\alpha_{\hat{n}} = 65°$. If $\alpha_{\hat{n}}$ were distributed uniformly, then 28% of the cases would occur in the range $65° \leq \alpha_{\hat{n}} \leq 90°$. That this is comparable to the 24% observed is coincidental, because a uniform distribution of $\alpha_{\hat{n}}$ is a very unlikely one for the interplanetary medium as an examination of Voyager 1 data for the first 150 days of 1981 shows.

As Lepping et al. (1982) discuss, Voyager 1 data for a period comparable to the Voyager 2 period do not reveal the presence of Jupiter's distant tail. [In that paper, however, there was an incorrect assertion that early in 1981 Voyager 1 was located only 4° away from the extended sun-Jupiter line. In fact, the spacecraft led Jupiter by about 14° in the ecliptic plane on day 1, 1981. From then until day 150 the sun-Jupiter-spacecraft angle varied from 165.8° to 162.6°, almost monotonically, so that Voyager 1 was always 15 1/2° (± 1 1/2°) away from the nominal (unaberrated) Jupiter tail axis over that period. This and the great Jupiter-to-spacecraft range are apparently the principal reasons why the tail was not observed at Voyager 1. Near alignment of the sun, Jupiter, and the spacecraft would have occurred during that period if the spacecraft had not departed from the ecliptic plane. It reached $\lesssim$ 13° in latitude with respect to Jupiter on day 150.]

In order to compare the Voyager 1 and 2 data for the related periods discussed here, a variance analysis of Voyager 1 magnetic field data for days 1-150 of 1981 was performed as described above for the Voyager 2 data. (See Appendix A for details on percentage of acceptable Voyager 1 data resulting from the analysis). Figure 6 shows the resulting distribution of minimum variance normals in terms of $\alpha_{\hat{n}}$ and heliographic $\lambda_{\hat{n}}$ and $\delta_{\hat{n}}$. The distribution is in striking contrast to that of Voyager 2, shown in Figure 5. The $\lambda_{\hat{n}}$ and

$\delta_{\hat{n}}$ distributions are now much narrower, and the former peaks at $\sim$ 180°, as expected at this distance from the sun. The slightly skewed (toward negative values) appearance of the $\delta_{\hat{n}}$ distribution is probably partially accounted for by the fact that the Voyager 1 spacecraft departed from Saturn and from the ecliptic plane over this period, as mentioned above. But the difference between the Voyager 1 and 2 variance analyses is displayed most effectively and dramatically by the $\alpha_{\hat{n}}$ distributions (recalling that $\alpha_{\hat{n}}$ is defined with respect to a Jupiter-spacecraft line and adjusts for angular displacements of both spacecraft from the sun-Jupiter line). Comparing the $\alpha_{\hat{n}}$ distributions from Figures 5 and 6 (solid curves only) we see a marked difference, especially in the larger angles, which are essentially absent in the Voyager 1 distribution. One can reasonably envision the Voyager 2 $\alpha_{\hat{n}}$ distribution being composed of one like that from Voyager 1 (solid curve) plus one having the shape of the dashed distribution, which is, in fact, the difference between the Voyager 1 and 2 $\alpha_{\hat{n}}$ distributions beyond $\alpha_{\hat{n}} = 40°$. If the dashed distribution is indicative of that associated with Jovian magnetotail phenomena, then our choice of a cut-off at $\alpha_{\hat{n}} = 65°$ in the Voyager 2 variance analysis (Appendix A) is conservative, allowing few contaminating points.

The bottom panel of Figure 4 shows the results of the Voyager 2 variance analysis. A vertical bar represents the percent of cases in a day for which our eigenvalue criteria are satisfied and for which $\alpha_{\hat{n}} > 65°$. Notice the generally good correlation of cases with the 'tail' regions of Figure 2, and with the low density (N) and low field (B) regions discussed above. It is especially interesting that high percentages often occur adjacent to apparent boundaries of the 'tail' regions as draped field would be expected to do. Similarly they occur at density gradients where the spacecraft is entering or leaving the tail. It is equally noteworthy that high percentages of $\alpha_{\hat{n}} > 65°$ often occur <u>throughout</u> 'tail' regions. From an examination of the most prominent events it appears that this is at least partly due to multiple tail or tail-filament encounters occurring throughout a given event, but some of this appears to occur when the spacecraft is <u>inside</u> the tail, i.e., where tail-lobe fields are commonly seen; detailed examination of the May 1981 (no. 5) event (discussed below) supports this view. Tail current sheets may tend to give $\alpha_{\hat{n}} \sim 90°$ at these distances. Alternatively, if the tail-field is oscillating in a transverse mode, either in latitude, longitude or a

combination, with periods in the neighborhood of our 12-hour analysis interval (or conceivably several times longer), then minimum variance normal directions would also occur near $\alpha_{\hat{n}} = 90°$. This tends to add support to the assertion by Kurth et al. (1982b) that large scale waves (periods of $\sim$ 2.5 days) exist within the tail. Clearly further analysis should be done on the question of waves.

For a final comparison of the magnetic field structure between the Voyager 1 and 2 data sets we present Voyager 1 data for the first 150 days of 1981 in Figure 7, in previously used formats. Specifically the top panel gives the percent of hours in a day for which the field has $\alpha < 30°$ or $> 150°$, and the bottom panel shows the percent of acceptable minimum variance normal estimates in a day for which $\alpha_{\hat{n}} > 65°$. As we see, when compared to the comparable Voyager 2 quantities in Figures 2 and 4, there is no evidence for the Jovian tail in the Voyager 1 MAG data at this time, as Lepping et al. (1982) reported using preliminary data; the final data give an even more definite result. Kurth et al. (1982b) support this assertion from an examination of the Voyager 1 PWS data.

Statistical Properties

Here we briefly examine some statistical properties of the magnetic field for the regions denoted TAIL, CORE and CONTROL (IMF-like magnetosheath fields) for 1981 as delineated in Figure 2. Tables 1 and 2 list the TAIL and CONTROL regions, respectively, and the CORE regions are given in Kurth et al. (1982b). Recall that these regions were defined in terms of PWS, PRA, and PLS data, but not by MAG data, in order to permit an independent study of the field in these regions. (For comparison Table 3 presents tail regions as determined by MAG data, where the direction of the field, $|\beta| \geq 60°$, is used as a discriminator; see Figure 3 for a definition of β.) Figure 8 shows percent histograms of the hourly average magnetic field in terms of the magnitude B, and heliographic longitude λ and latitude δ, as well as the pythagorean mean RMS (SIG). N is the number of hour averages used for each histogram; for example, N=1651 is the number of hours summed over all the control groups of Figure 2. In the case of the λ-panels, data from $-45°$ to $135°$ were superimposed on those from $135°$ to $315°$, since our concern is less with the sense of the field than with

particular alignments. The solid vertical arrows represent predicted values based on a Parker model of the IMF at a distance of 7,000 R_J downstream from Jupiter (i.e., at $\sim$ 8 AU from the sun). The dashed vertical arrows are values for λ and δ that might be expected for a simple, well-behaved tail field aligned with the solar wind flow direction. Before discussing these distributions, it should be pointed out that there are far fewer hourly averages in the CORE set (N = 217) than in the other two sets: N (tail) = 1503 and N (control) = 1651; thus, the derived statistical properties of the CORE set are less certain.

The CONTROL set is well behaved, even if slightly broadly distributed in δ and SIG. In particular, the peaks in B, λ and δ lie close to expected values. These distributions provide a set against which we can compare the TAIL and CORE distributions. The CORE set is markedly different from the CONTROL set: the CORE B-distribution is sharp and peaks at a value about half the Parker predictions, while the λ-distribution is somewhat broad but peaks at 0°, 180° as expected. The δ-distribution is the only real surprise in that it appears to be flat or possibly bimodal, neither apparent peak being at $\sim$ 0° as a simple model would predict. It may be that the poorer CORE statistics are at least partially responsible for the odd appearance of the δ-distribution. The SIG-distribution is interesting in that it is sharper and peaks at a lower value ($\sim$ 0.03 nT) than that for the CONTROL set.

In many respects the TAIL is intermediate between the CONTROL and CORE sets. In particular, the B-distribution peaks midway between the values of the peaks for the other two sets, although it is narrow like the CORE B-distribution. The λ-distribution has no discernable peak and is roughly comparable to a mixture of the other two λ-distributions. The δ-distribution, however, is similar to that of the CONTROL set, and the SIG-distribution is comparable, to, if not sharper than, that of the CONTROL.

Possibly the mixed appearance of the TAIL set is due to the difficulty in identifying the exact boundaries of each event and partially to the long duration of the (1 hour) averages used in the analysis, but it is very likely that the tail field has a complex structure, i.e., it is not simply lobe-like. Examination of the individual events seems to confirm this. In this regard,

distributions of B, λ,δ and SIG were developed for each event separately before the summed distributions were formed, and for the most part, when statistically significant, the individual distributions resembled those shown in Figure 8.

To summarize, the inner tail regions, presumably the CORE regions, have on average a lobe-like magnetic field structure, but often they are much more complex, and in particular possess unusually high field latitudes. The magnitude of the field in these regions is clearly lower, by a factor of $\sim$ 2 on average, than the external magnetosheath field. This would be unexpected for an expanding tail, which appears to be its state for many of these events, or for a quasi-steady portion of the tail, assuming the tail B-field pressure is the principal contributor to the internal pressure; this apparent paradox will be discussed below. These inner tail regions have a much narrower spread of field magnitudes and SIG's than the external field. The TAIL set has properties of both the CORE and CONTROL sets implying that it may indeed be composed of true tail fields plus magnetosheath fields. This should be expected if the tail has some significant filamentary structure, allowing samples of both types of regions to be observed over the many days of an 'event'.

In the following correlation analyses it will be convenient to define the direction of the magnetic field in terms of a latitude angle β, which is that angle between the magnetic field and the plane perpendicular to the Jupiter-spacecraft line, with vertex at the spacecraft, as shown in Figure 3. Hence, according to our earlier definition of α, we see that $\beta = 90^\circ - \alpha$. As discussed earlier, changes in the solar wind apparently are responsible for the quasi-periodic appearance of the distant tail sightings, especially for the 1981 events, where here a sighting refers to an entire event and not simply part of an event, such as a filament encounter. To test quantitatively our impression that the various events arrived quasi-periodically according to variations in the solar wind pressure, an autocorrelation analysis was performed on the Voyager 2 magnetic field data for the first 230 days of 1981. In particular, 12-hour averages of $|\beta|$ were autocorrelated for three cases: (1) $|\beta| > 45^\circ$ (before averaging), (2) $|\beta| < 30^\circ$ (before averaging), i.e., the 'IMF' case, and (3) for all $|\beta|$. The top two panels in Figure 9 show the

results of these analyses for cases (1) and (2) in terms of the correlation coefficient vs day lag, with case (3) results displayed in both panels for comparison. Notice that both cases (1) and (3) are in rather good agreement at all lags and have a distinguishable peak at a lag of 25 days, which is the sidereal solar rotation period; no adjustment of this period because of spacecraft longitudinal motion is necessary at these distances from the sun. [As mentioned above a simple average of the intervals between successive 1981 events yields an average event-periodicity of 26.5 days (Lepping et al., 1982), in support of the 25-day peak derived here.] By contrast, case (2) shows no noticeable agreement with case (3) and few prominent peaks, the one at 25 days being not significantly higher than others.

We conclude that the field direction at this time is generally [case (3)] influenced by quasi-periodic solar wind pressure structure, as presumed, and that using a data set in which a tail encounter is more likely [case (1)] yields the conclusion that the occurrence of tail-like fields at the spacecraft's location is similarly influenced by corotation effects. By contrast, using the set in which a tail encounter is very unlikely [case (2)] shows a very weak, if not negligible, relationship to corotating structure.

The correlation of high amplitude PRA continuum radiation at 1.2 kHz with lobe-like magnetic fields as shown in Figure 2 was tested quantitatively by performing a cross-correlation analysis of MAG $|\beta|$ with PRA amplitude at this frequency using again data for the first 230 days of 1981. In particular, only data with $|\beta| > 45°$ were retained and then averaged over 12-hours. Likewise only PRA data with amplitudes greater than 1.5 dB were retained and similarly averaged. The correlation coefficient vs day lag resulting from this analysis is shown by the solid curve in the bottom panel of Figure 9. Prominent peaks occur at 0 and near $\pm$ 25 days lag, as expected, confirming the apparently good correlation of the MAG and PRA data.

The May Event

In Figure 10 we display 30 days of magnetic field, plasma, and PRA continuum radiation data around the time of the May 1981 event (no. 5). In the figure "TAIL" covers the period from day 140, hour 21 to day 148, hour 20

according to Table 1, and "CORE" covers the period from day 144, hour 8 to day 145, hour 0 (Kurth et al., 1982b). Probably the most striking feature of Figure 10 is the approximate symmetry and good correlations among the 1.2 kHz noise level, V, N (and therefore $m_p MV^2$), and B. Even the CORE is closely centered in the TAIL region. It occurs at a time when the field reaches the lowest ($\sim$ 0.1 nT) sustained ($\sim$ 1 day) value, and interestingly this is when the field direction changes from $\beta > 60°$ (lower dashed line) to $\beta < -60°$ (upper dashed line), peaking at day 145, hour 3. This directional variation indicates a change from a clearly southern lobe field, which lasted $\sim$ 3 1/3 days, to a brief period in the northern lobe observed on day 145; the region between the β-curve and the $+60°$ dashed line is darkened for emphasis. Across the apparent inbound boundary, centered on $\sim$ hour 21 of day 140 (vertical dashed line), B significantly increases, N drops moderately, V continues to drop slowly, and β abruptly changes from a variable sheath-like value to the southern lobe value at the beginning of the darkened region. Because of these characteristics generally and because the PRA continuum is confined within this boundary, we will tentatively consider it to be a magnetopause. The "end" of the tail region is not so distinct in either the PLS or MAG data; the latter appear to indicate a slightly earlier termination by $\sim$ 1 day with a further brief (perhaps filament) encounter on day 152 where the field is northern lobe-like. The large velocity gradient occurring early on day 153 appears to be a solar wind feature.

The quantity $\beta_{\hat{n}}$ (dotted curve in the β-panel) is the latitude angle (see Figure 3) of the minimum variance normal of magnetic field variations based on hour averages over 12-hour analysis intervals. (The same criteria as those used in obtaining $\hat{n}$ for Figure 4 were employed here; see Appendix A for the criteria.) By definition $\beta_{\hat{n}}$ must lie in the range $-90° \leq \beta_{\hat{n}} \leq 0°$. The most interesting values of $\beta_{\hat{n}}$ are those near 0° (center line of the panel), representing either normals produced by magnetic fields draped around the tail boundary (or mimicking such behavior), or, if internal to the tail, indicating the possibility of plane-polarized variations of the field transverse to the tail axis, i.e., field variations in any plane which approximately contains the tail axis. This appears to be the case for the period from early day 141 to early 142, and again at various times throughout days 145 and 146. Draped fields occur on day 136, and probably on 130, and maybe on early 140 and late 152.

Notice the overall qualitative tendency for $\beta_{\hat{n}}$ to track β with a 60° to 90° displacement throughout the 30-day period regardless of whether the spacecraft is in the distant magnetosheath, draped field region of the magnetosheath, or the tail. This indicates a general tendency for the maximum variation plane to contain the average field within $\sim$ 30°. This is especially noteworthy, since the variance method employed is that of Sonnerup and Cahill (1967) which uses difference-fields throughout an analysis interval (i.e., $\Delta\vec{B}_i = \Delta\vec{B}_i - \langle\vec{B}\rangle$, where $\langle\vec{B}\rangle$ is an average over the analysis interval) rather than using the field, $\vec{B}_i$, directly, which would more likely give such a result.

Probably the most puzzling characteristic of these data is their apparent difficulty in explaining, even qualitatively, how the distant tail is able to hold off the external pressure imparted normal to its boundary by the magnetosheath plasma. This total external pressure, P^E, should be the sum of the normal component of the ram pressure, the external tangential magnetic field pressure and the thermal pressure primarily produced by electrons and protons. Under static conditions P^E must be balanced by the internal pressure, P^I, which is expected to be composed predominantly of magnetic pressure ($B^2/8\pi$) of the tail field, but also to consist of thermal plasma pressure and possibly of energetic particle pressure. The internal thermal plasma pressure as observed by PLS is much too low to balance P^E alone as pointed out by Kurth et al. (1982b). Also the internal particle pressure for ions > 6 keV is unknown. Below (Discussion) we argue that an internal bulk flow pressure (m_pNV^2) probably plays a role in providing pressure balance in the steady state or the proper pressure imbalance under more common dynamic conditions. (Notice in Figure 10 that the change in m_pNV^2 across the inbound boundary on day 140 is not very sharp, and that therefore the internal bulk flow pressure may be significant.) In fact, static conditions are rarely (if ever) observed in any of the tail sightings, probably because the sightings are the result of tail motion or expansion to the position of the spacecraft as discussed by Lepping et al. (1982) and Kurth et al. (1982b). The least we should expect then is that, upon first entering the tail, $B^2/8\pi$ should increase at least slightly across the boundary as it does on day 140, and upon exiting it should increase again (or not significantly change, but should not likely decrease), since the tail is probably collapsing and $P^E > P^I$. A

significant increase in B is not apparent at or near the 'end' of the TAIL interval, but does occur shortly thereafter. The important issue of pressure imbalance across the tail boundary is treated more fully and quantitatively in the Discussion.

A variance analysis (Sonnerup and Cahill, 1967) of the field during the broad transition zone of the inbound tail boundary from 2000 to 2120 UT of day 140 was performed using 48-s averages, in order to confirm its identification as a magnetopause current sheet. The resulting minimum variance normal direction was $\lambda_{\hat{n}} = 94^\circ$ and $\delta_{\hat{n}} = 39^\circ$. The longitude $\lambda_{\hat{n}}$ is reasonably consistent with what is expected (85°) at the location of event 5 according to Figure 1. The eigenvalue ratios were acceptable: $E_1/E_2 = 3.6$ and $E_2/E_3 = 2.6$. And the angle across the discontinuity zone in the discontinuity plane ω was 81°. If we assume that the boundary is a tangential discontinuity and the variance analysis of Siscoe et al. (1968) is used for this same interval, then the resulting minimum variance normal direction is $\lambda'_{\hat{n}} = 88^\circ$ and $\delta'_{\hat{n}} = 33^\circ$, which is in even closer agreement with the expected longitude. The eigenvalue ratios are significantly better in this case: $E'_1/E'_2 = 4.4$ and $E'_2/E'_3 = 8.6$. Again the angle ω has a reasonable value of 80°. In either case the latitude of the normal was positive and well out of the ecliptic plane, which is what is expected if the spacecraft enters the southern lobe of the tail at moderately high (negative) latitudes; note that the normal is defined such that it points inward at the boundary. This is consistent with Figure 10 which shows β's $> +60^\circ$ (darkened region) after entering the tail. Hence, the inbound magnetopause was very broad, had characteristics of a tangential discontinuity, and had a properly directed normal, confirming its identification.

Discussion

We discuss here three major issues in the following order: (1) the structure and dynamics of the distant tail and how they are related to seeing it approximately every 25 days, (2) the question of pressure balance, or imbalance across the boundary of the distant tail in relation to observations, and (3) the possibility of Saturn being in Jupiter's tail during the Voyager 2 encounter.

1. Structure and Dynamics. It is planned that a future paper will comprehensively discuss the dynamics of the distant tail, but here we briefly develop a preliminary and qualitative view. From our findings we know that the solar wind pressure structure (Burlaga, 1983b) causes near-periodic tail variations resulting in the tail engulfing Voyager 2 approximately every 25 days. In particular we believe these variations primarily are manifested as periodic expansions and contractions, based mainly on the variations of the magnitude of the magnetic field within the tail. Also, except for occasions when major segments possibly break off due to field line merging (see Kurth et al., 1982b; their Figure 9), we assume that the tail is generally much longer (probably many times the observed 9,000 R_J) than the radial peak-to-peak scale length of the solar wind pressure variations, which average $\sim$ 13,000 R_J; Grzedzielski et al. (1981) estimate the Jovian tail length to be 7-15 AU, i.e., (15-32) x 10^3 R_J. Therefore, it is not likely that the tail ever assumes a uniform or simple configuration. It is likely to have a quasi-periodically variable width like a string of sausages, as shown in Figure 11, where the narrow cross-sections are associated with high pressure solar wind regions and the large cross-sections with low pressure regions. The tail boundary may then be envisioned dynamically, to first approximation, as a traveling wave with period $\sim$ 25 days. We also expect secondarily some lateral motion due to pressure differences across the tail and to solar wind flow direction changes. [If the earth's magnetotail is sufficiently long, it too would have such a sausage-string shape, for the same reasons, but in any case it should suffer cross-sectional changes dependent on external pressure changes.] We still cannot rule out the possibility, at least on some occasions, that the Jovian tail experiences lateral motion as a primary mode.

Apparently supporting our finding of a 25-day periodicity in the tail's motion is a report by Pyle and Simpson (1977) that Pioneer 10 plasma data (communicated to them by J. Wolfe, principal investigator) revealed that the solar wind "disappeared" in two intervals, separated by 24 days in early 1976, when the spacecraft was downstream from Jupiter by about 4 1/2 AU. They did not speculate on the origin or mechanism for these solar wind dropouts but suggested they may have been due to the recurring interaction of a solar wind 'corotating interaction region' with the Jovian magnetotail. It is possible that the Pioneer 10 plasma "dropouts" were signatures of the central, very low density portions of an expanded tail, as described above.

Voyager 2 PWS and PLS observations (Kurth et al., 1981, 1982b) also indicate that we should expect some further complexity of Jovian tail in the form of filamentary structure. Our observations generally seem to support this view; see especially events 1 and 4 in Figure 2. However, the tail apparently is not dominated by filamentary structure at the distances observed ($5\text{-}9 \times 10^3$ R_J), at least not commonly, or the encounter regions would have had a more random occurrence pattern. On the contrary, most tail regions were fairly well defined, lasted many days, and had bipolar, lobe-like magnetic field structures; but as the statistical study showed, they also contained other complicated field structures. In summary, according to this view the spacecraft is found inside or outside of a sausage-string shaped, slightly filamentary, magnetotail depending on how close it is to the Sun-Jupiter line and on the phase of the solar wind total pressure variation as discussed in connection with Figure 4. This is consistent with the "time symmetry" model of Lepping et al. (1982).

Figure 12 (upper portion) shows a summary cartoon of a portion of the tail out to the orbit of Saturn in a Jupiter orbital plane view. Also shown are the major tail encounter points along the Voyager 2 trajectory which on average occur every 25 days, twice the time it takes for the solar wind total pressure to wax and wane as experienced by the tail boundary. The sketch is shown for the case when the external pressure is at maximum near Jupiter (shaded area) and for when the external pressure is at a minimum near Jupiter (dashed curve). In the bottom portion of the figure idealized oval cross-sectional shapes are shown for the two situations, where we speculate that the north-south total pressure exceeds the east-west total pressure due to the significant contribution of the external $\vec{B}$ pressure anisotropy from a highly probable Parker-spiral field (L. Burlaga, private communication). Such oval cross-sectional shapes are expected to be likely at all distances from Jupiter, since in general the solar wind plasma beta is relatively low over its entire length, but the degree of north-south flattening is unknown. The same idea was suggested for the Earth's magnetotail by Michel and Dessler (1970), but it probably should apply beyond a few hundred Earth radii downstream from Earth (A. Dessler, private communication).

Owing then to the possibility of the shorter north-south dimension and to the fact that Voyager 2 was above the Jupiter orbital plane, it is not surprising that the Jovian tail avoided the spacecraft during the contraction periods, even when the spacecraft was in the vicinity of the expected tail axis. Only during event no. 4 should we expect some failure of this picture, since at that time the spacecraft was quite close to the nominal aberrated tail axis (320 R_J) and encountering it would have been hard to avoid; notice in this regard the complex structure of this event in Figure 2.

2. Pressure Balance. Since a survey plot of the magnetic field magnitude (Figure 4) shows that low fields are highly correlated with the encounter intervals, it appears that the conventional view of the internal magnetic field pressure of the tail balancing the net external pressure does not hold for the distant Jovian tail at these distances. One is therefore tempted to search for a tail constituent, such as energetic particles, to account for the missing internal pressure. However, we believe that a simple modification of the 'conventional view' is the correct one, and that under quasi-steady conditions, and excluding the core, the internal field pressure plus internal tailward bulk plasma flow pressure does balance the external pressure, which consists of a component of the solar wind ram pressure, the $\vec{B}$ pressure, and to a lesser degree the thermal pressure. And as we qualitatively argued for the May 1981 (no. 5) event, at the tail boundary crossings the field pressure changes had the correct signs. The core regions are not understood; we will return to this issue at the end of the Summary. With this qualification the apparent dilemma is solved, if it is realized that in general: (a) the survey plot (Figure 4) is mainly indicative of a gross overview of solar wind structure with some modification due to the occasional presence of the tail, and that a much finer scale view must be taken in examining the pressure-change across a tail boundary; (b) a tail sighting occurs when there is a pressure imbalance across the tail boundary; (c) if the tail sighting is principally due to expansion of the tail to the spacecraft's position, then when the spacecraft enters the tail B should increase, even if only slightly, to account for the expansion, and detailed study has shown it does so within our ability to determine boundaries for all of the prominent events already examined [shown in Figure 3 mid-day 49, 1981, in Lepping et al. (1982) for event no. 2; in Figure 4, early on day 67, in Kurth et al. (1982b) for event

no. 3; and in Figure 10, late day 140, in this paper for event no. 5]; (d) when the spacecraft exits during the subsequent tail contraction, B should also increase, as both the survey plot (Figure 4) and finer scale plots show, whenever the outbound boundary is clearly identified; (e) a non-negligible bulk plasma pressure ($m_p NV^2$) exists within the tail regions, since both N and V are usually significant throughout most of these regions (excluding the core), as shown in Figures 4 and 10; and (f) there is probably a small thermal pressure change across the tail boundary. There is no evidence yet available that significant energetic particle pressure exists within the distant tail, but its presence appears necessary to explain the existence of the core regions, since B and N (thermal plasma) are so low in the cores.

We believe that the plasma flowing within the tail is the result of solar wind plasma entering Jupiter's magnetosphere, possibly at cusp regions as at Earth, and probably also through gradual diffusion across the tail boundary (magnetopause) or more rapidly at regions of the magnetopause where there is a field locally perpendicular to the boundary (rotational discontinuity). Based on knowledge of the earth's case (Hones et al., 1972 and Sckopke and Paschmann, 1978), this combined 'mantle/boundary layer' plasma may be expected to fill almost the entire cross-section of the tail (excluding the core) at great distances and have characteristics similar to the adjacent magnetosheath plasma, but be slightly slower and slightly less dense, as we observe in Jupiter's distant tail. However, by contrast in the tail lobe region close to earth (i.e., $\lesssim 35\ R_E$) plasma densities are very low, typical minimum values being $\sim 0.01\ cm^{-3}$ (R. R. Anderson, private communication). The densities that we are encountering in Jupiter's distant tail range from slightly less than $0.1\ cm^{-3}$ to $< 10^{-3}\ cm^{-3}$ (core regions) occasionally, which contrast markedly with the exceedingly low densities in the tail lobe region close to Jupiter ($\lesssim$ $155\ R_J$) inferred by Gurnett et al. (1980) to be $< 10^{-5}\ cm^{-3}$.

Let us examine the inbound magnetopause crossing on day 140 of event 5 (Figure 10) in light of these remarks. Since the tail is probably expanding at this time, the following total pressure expression should hold across the inbound boundary in an inertial frame (approximately the spacecraft frame); recall that $\vec{B}$ was locally tangential to both sides of this boundary:

$$P_B^I + P_R^I \sin^2 \sigma^I + P_T^I \gtrsim P_B^E + P_R^E \sin^2 \sigma^E + P_T^E, \qquad (1)$$

where P_B, P_R, and P_T are the magnetic pressure ($B^2/8\pi$), the bulk plasma (ram) pressure, and the thermal pressure due to protons and electrons, respectively, and σ is the acute angle between the bulk plasma flow direction and the local boundary; I and E refer to regions immediately adjacent to the boundary and internal and external to it, respectively. Rearranging terms and defining $\Delta P_B \equiv P_B^I - P_B^E$, clearly a positive quantity for this boundary, and $\Delta P_T \equiv P_T^I - P_T^E$, yields:

$$\Delta P_T + \Delta P_B \gtrsim P_R^E \sin^2 \sigma^E - P_R^I \sin^2 \sigma^I \qquad (2)$$

We are attempting to find a <u>limit</u> on the angle of attack σ^E for the external flowing plasma for the case where the internal flow pressure is ignored, so we will drop the last term. It will probably be small compared to $P_R^E \sin^2 \sigma^E$, since $P_R^E > P_R^I$ and σ^E is probably much larger than σ^I, which is unknown. The value of ΔP_T is not well determined, but a useful estimate can be made. The limit on σ^E can then be expressed as

$$\sigma^E \lesssim \sin^{-1} [(\Delta P_T + \Delta P_B)/P_R^E]^{1/2} \qquad (3)$$

Examination of Figure 10 shows that $\Delta P_B \lesssim 8.4 \times 10^{-13}$ dynes cm^{-2} and $P_R^E \lesssim$ 5-20 $\times 10^{-11}$ dynes cm^{-2}, and estimates of the thermal pressure show that $\Delta P_T \lesssim -4.6 \times 10^{-13}$ dynes cm^{-2}. Hence, we find that

$$\sigma^E \lesssim 4^{\circ} \pm 1.5^{\circ}$$

Notice that Figure 1 (top panel) shows that a line from event no. 5 to Jupiter makes an angle of $\sim 6^{\circ}$ with the sun-Jupiter line, a reasonable expectation for σ^E, if the solar wind was flowing approximately radially from the sun at this time; our estimated limit on σ^E is slightly smaller. Our main point, however, is that it is not difficult for the estimated net internal pressure to overcome the net external pressure for the field changes observed at times when the tail is sighted. Moreover a significant amount of internal boundary layer plasma is flowing more or less parallel to the tail boundary, the magnetopause, so as to increase further the total internal pressure. Outbound the

situation is quite different in that the inequality reverses, $B^2/8\pi$ again increases with time across the boundary along with the ram pressure, and the tail collapses. The collapse continues until this 'portion' of the tail reaches a brief equilibrium state in which total internal/external pressures balance. This is not seen at the spacecraft which is well outside of the tail by this time.

3. Saturn in the Jovian Tail? In our previous discussion of this question (Lepping et al., 1982) we expressed some doubts about this possibility. Since then several new facts and observations have lead us to believe that it is quite likely that Saturn was in Jupiter's tail during most of the Voyager 2 Saturn encounter. First, Kurth et al. (1982a) have recently discovered nonthermal continuum radiation in Saturn's magnetosphere in the Voyagers 1 and 2 PWS high resolution wideband observations; hence, one negative argument is removed. However, since both Voyagers 1 and 2 detected continuum radiation at Saturn, we do not have a strong positive argument in this respect either; the radiation may simply be Saturn-related. Second, as mentioned above, Scarf et al. (1983) report on several certain post-Saturn Voyager 2 Jovian tail encounters. Third, a statistical study using Voyager PLS data (see discussion by Kurth et al., 1982a) revealed that a decrease of the solar wind ram pressure alone would not be expected to permit Saturn's magnetosphere to expand as far as it apparently did for as long as it apparently did ($\sim$4.5 days) during the Voyager 2 encounter. In addition, Behannon et al. (1983) show that the probability of Saturn being in Jupiter's tail for the entire period of the proposed 4.5 days was as great as 0.35 that for a typical (i.e., on average) 1981 Jovian tail encounter. (A few tail encounters that were well identified had even lower relative probabilities of occurrence according to this analysis.) Their estimate was based on a simple argument using the frequency distribution of the pre-encounter tail events plus two post-Saturn events (F. Scarf, private communication), and on the timing of Saturn's magnetospheric encounter, all in solar-rotation-day space. Based on the above arguments alone it is moderately probable that such an event did occur, but the evidence is indirect. Recently, however, Desch (1983) has added considerable credence to this possibility using direct evidence. He has deduced that Saturn's immersion into the tail probably started at about hour 10 of day 237, 1981, and lasted approximately 5 days,

based on a dramatic decrease and subsequent recovery in Saturn Kilometric Radiation (SKR) during the encounter (i.e., an extended emission dropout) and on correlations of similar dropouts, observed over a period of 4 months pre-Saturn, with known Jovian tail encounters by Voyager 2 as identified by our present paper and Kurth et al. (1982b). Desch reasons that interpretating the pre-Saturn dropouts as the radio signatures of successive Saturn immersions into Jupiter's tail is consistent with the fact that the SKR source is driven by external ram pressure (Desch and Rucker, 1983), so that SKR dropouts should occur in response to density decreases that occur within the tail and especially in the tail's core, as we have shown. Also Voyager 2 was radially upstream of Saturn during this extended period. Hence, based on all of the evidence, direct and indirect, we believe it is quite likely that Saturn was in Jupiter's tail during most of the Voyager 2 encounter.

Summary

We now summarize our findings, first for the well-established results and then for the less well-established conclusions or speculations.

Well-established:

- Jupiter's distant tail was detected out to at least 9,000 R_J by PWS, PLS, PRA, and MAG experiments onboard Voyager 2.

- Auto- and cross-correlation analyses determine an approximate periodicity of the tail encounters of 25 days, indicating that solar wind structure is reponsible for controlling tail motion. (The average time between event centers for 1981 was $\langle \Delta t \rangle$ = 26.5 days.)

- All core events lie within a cone angle of $\sim 12^\circ$ with respect to the Sun-Jupiter axis and are most prominent and long lasting for the several events near the time when Voyager 2 was closest to the aberrated tail axis (day 105, 1981); recent observations of post-Saturn events may increase the cone angle moderately (Scarf et al., 1983).

- Most prominent events display the expected bipolar and lobe-like nature of the tail field, but some anomalous $\vec{B}$ directions exist in the core and especially in the tail regions as a whole, indicating complexity of internal structure.

- Magnetic field variance analyses indicate that field line draping around the tail boundary is common and that transverse field variations occur within the tail and/or tail current sheets. It is interesting in this regard that Kurth et al. (1982b) point out the presence of large scale waves (with periods of $\sim$ 2.5 days) within the tail.

- A considerable flux of plasma is observed within the tail as is evidenced by only moderate changes in V and N across a tail boundary as determined by the MAG and wave data. However, V and N drop precipitiously to very low values upon entering the core.

Less Well-established:

- Some filamentary structure of the tail is apparent based on the occurrence distribution of events and their structure, and according to arguments by Kurth et al. (1981, 1982b).

- The principal motion of the tail is $\sim$ 25-day periodic cross-sectional expansion and contraction. This belief is based mainly on the behavior of the magnitude variation of $\vec{B}$ on both the large and small scale; also see Kurth et al. (1982b) who speculate on this probability. This is consistent with the fact that the solar wind total pressure varies with an average 25-day period at these distances. [Also see supporting information from Pioneer 10 plasma data reported by Pyle and Simpson (1977) that possibly two Jovian tail encounters, separated by 24 days, occurred when the spacecraft was downstream from Jupiter by about 4 1/2 AU.] Flapping (bulk lateral motion) probably also occurs, due to changes in solar wind flow direction and to external pressure differentials across the tail.

- The pressure imbalance necessary to control the tail expansion or contraction is apparently controlled by bulk plasma flow pressure and by the magnetic field pressure on <u>both</u> sides of the tail boundary. The presence of such flowing plasma within the distant tail is a natural consequence of the existence of tailward flowing mantle/boundary layer plasma within the near-planet tail (Gurnett et al., 1980), plus plasma that has diffused into the tail from the magnetosheath or penetrated at regions of the magnetopause where $\vec{B}$ is locally normal.

- The tail is probably many times longer than the greatest distance at which it has been observed and therefore has a sausage-string appearance due to solar wind pressure variations (Figure 11). The cross-section at any given distance is probably oval-shaped with a north-south dimension shorter than the east-west dimension, due to external $\vec{B}$ pressure anisotropy (L. Burlaga, private communication).

- Based on indirect evidence it is at least moderately probable that Saturn was in Jupiter's tail during the Voyager 2 Saturn encounter. Recent direct evidence from Saturn Kilometric Radiation data adds considerable weight to the possibility (Desch, 1983).

We mention here outstanding problems that barely have been addressed in this work. Presently the composition of the tail plasma is unknown and without such knowledge computations of internal pressure will be in some doubt, and the core regions need further analysis and understanding. Are the cores, where N is very low, analogous to the earth's plasma sheet in that they appear to occur at 'neutral sheet' regions where B is also low? Must they contain low density hot plasma to provide the needed internal pressure to resist collapse? For example, as pointed out by Kurth et al. (1982b) an as yet unmeasured plasma component in the core with a density of $\sim 10^{-3}$ cm^{-3} and a temperature of $\sim$10 keV would be sufficient to provide the needed internal pressure. These questions probably have an affirmative answer, but clearly more must be done in this area.

Appendix A

To supplement the text on the Voyager 1 and 2 (survey) magnetic field variance analyses, specific information on percent of useful data and other restrictions are given below.

Only minimum variance normals for which $E_1/E_2 \leq 30$ and $E_2/E_3 \geq 2.0$ were retained in the survey variance analyses, where E_1, E_2, and E_3 are the maximum, intermediate, and minimum eigenvalues (variances), respectively; all others were of too poor a quality to define accurately the maximum variance plane (see Lepping and Behannon, 1980). Optimum Voyager 2 results occur for a separation angle of $\alpha_{\hat{n}} \sim 65°$, i.e., for $\alpha_{\hat{n}} \geq 65°$ the derived normals appear to be predominantly tail-associated. This is consistent with lobe-like fields occurring predominantly for $\alpha < 30°$ and $\alpha > 150°$, since the $\hat{n}$'s should be approximately perpendicular to these fields via the draping mechanism. Out of 287 days, 1919 normal estimates (84%) were obtained; data gaps precluded getting the full 2296 (24/3 x 287) possible. Of these 1919 estimates, 1304 cases, or 68%, remained after elimination on the basis of the two eigenvalue ratio criteria.

For Voyager 1, out of the 150 days, 964 minimum variance normal estimates resulted, i.e., 80% of the attempted 1200 estimates. Of these 964 estimates 590 cases, or 61%, remained after elimination on the basis of the eigenvalue ratio criteria, and of these only 7% satisfied $\alpha_{\hat{n}} > 65°$.

Acknowledgments

We wish to thank Joe Alexander, Len Burlaga and Norm Ness for reading the manuscript and for making helpful suggestions. We are grateful to Fred Scarf for pointing out the existence of post-Saturn Voyager 2 Jovian tail candidates and to Mike Kaiser for his generous help in expediting the handling of the Voyager PRA data with the assistance of Bridget Razzaghinejad. We thank one of the referees for asking the right question about the results from Voyager 1 which helped us to make an important correction. We also thank Bill Mish and his entire data processing team, all of whom contributed in various ways to this study, and Omer Divers (JPL) for obtaining useful Voyager trajectory

information for us. We acknowledge the general support of Norm Ness and Herb Bridge, the Voyager MAG and PLS principal investigators. Research at MIT was supported by a NASA grant through Contract NGL 22-009-015. The research at the University of Iowa was supported by NASA through contract 954013 with the Jet Propulsion Laboratory and by Grant NAGW-337 from NASA Headquarters.

References

Behannon, K. W., Mapping of the earth's bow shock and magnetic tail by Explorer 33, J. Geophys. Res., 73, 907, 1968.

Behannon, K. W., L. F. Burlaga, and N. F. Ness, The Jovian magnetotail and its current sheet, J. Geophys. Res., 86, 8385, 1981.

Behannon, K. W., R. P. Lepping, and N. F. Ness, The structure and dynamics of Saturn's outer magnetosphere and boundaries, J. Geophys. Res., this issue, 1983.

Belcher, J. W., H. S. Bridge, A. J. Lazarus, and J. D. Sullivan, Preliminary results from the Voyager solar wind experiment, Solar Wind Four, ed. H. Rosenbauer, proceedings of conference, Burghausen (28 August - 1 September 1978), October 1981.

Burlaga, L. F., Heliospheric magnetic fields and plasmas, Rev. Geophys. Space Phys., in press, 1983a.

Burlaga, L. F., Corotating pressure waves without streams, J. Geophys. Res., in press, 1983b.

Collard, H. R., J. D. Mihalov, and J. H. Wolfe, Radial variation of the solar wind speed between 1 and 15 AU, J. Geophys. Res., 87, 2203, 1982.

Desch, M. D., Radio emission signature of Saturn immersions in Jupiter's tail, J. Geophys. Res., in press, 1983.

Desch, M. D. and H. O. Rucker, The relationship between Saturn kilometric radiation and the solar wind, J. Geophys. Res., in press, 1983.

Eastman, T. E., The plasma boundary layer and magnetopause layer of the earth's magnetosphere, Ph.D. Thesis, U. of Alaska, Los Alamos Scientific Laboratory preprint LA-7842-T, 1979.

Fairfield, D. H., The ordered magnetic field of the magnetosheath, J. Geophys. Res., 72, 5865, 1967.

Goertz, C. K., The orientation and motion of the predawn current sheet and Jupiter's magnetotail, J. Geophys. Res., 86, 8429, 1981.

Grzedzielski, S., W. Macek, and P. Oberc, Expected immersion of Saturn's magnetosphere in the Jovian magnetic tail, Nature, 292, 615, 1981.

Gurnett, D. A., W. S. Kurth, and F. L. Scarf, Plasma wave observations near Jupiter: Initial results from Voyager 2, Science, 206, 987, 1979.

Gurnett, D. A., W. S. Kurth, and F. L. Scarf, The structure of the Jovian magnetotail from plasma wave observations, Geophys. Res. Lett., 7, 53, 1980.

Hones, E. W. Jr., J. R. Asbridge, S. J. Bame, M. D. Montgomery, S. Singer, and S.-I. Akasofu, Measurements of magnetotail plasma flow made with Vela 4B, J. Geophys. Res., 77, 5503, 1972.

Intriligator, D. S., H. R. Collard, J. P. Mihalov, O. L. Vaisberg and J. H. Wolfe, Evidence for earth magnetospheric tail associated phenomena at 3100 R_E, Geophys. Res. Lett., 6, 585, 1979.

Kurth, W. S., D. A. Gurnett, F. L. Scarf, R. L. Poynter, and J. P. Sullivan, Voyager observations of Jupiter's distant magnetotail, J. Geophys. Res., 86, 8402, 1981.

Kurth, W. S., F. L. Scarf, J. P. Sullivan, and D. A. Gurnett, Detection of nonthermal continuum radiation in Saturn's magnetosphere, Geophys. Res. Lett., 9, 889, 1982a.

Kurth, W. S., J. D. Sullivan, D. A. Gurnett, F. L. Scarf, H. S. Bridge, and E. C. Sittler, Jr., Observations of Jupiter's distant magnetotail and wake, J. Geophys. Res., 87, 10373, 1982b.

Lepping, R. P. and K. W. Behannon, Magnetic field directional discontinuities: 1. Minimum variance errors, J. Geophys. Res., 85, 4695, 1980.

Lepping, R. P., L. F. Burlaga, M. D. Desch, and L. W. Klein, Evidence for a distant (> 8,700 R_J) Jovian magnetotail, Geophys. Res. Lett., 9, 885, 1982.

Lepping, R. P., L. F. Burlaga, L. W. Klein, J. M. Jessen, and C. C. Goodrich, Observations of the magnetic field and plasma flow in Jupiter's magnetosheath, J. Geophys. Res., 86, 8141, 1981.

Michel, F. C. and A. J. Dessler, Diffusive entry of solar-flare particles into geomagnetic tail, J. Geophys. Res., 75, 6061, 1970.

Ness, N. F., The earth's magnetic tail, J. Geophys. Res., 70, 2989, 1965.

Ness, N. F., The geomagnetic tail, Rev. Geophys. Space Phys., 7, 97, 1969.

Ness, N. F., M. H. Acuña, R. P. Lepping, K. W. Behannon, L. F. Burlaga, and F. M. Neubauer, Jupiter's magnetic tail, Nature, 280, 799, 1979.

Pyle, K. R. and J. A. Simpson, The Jovian relativistic electron distribution in interplanetary space from 1 to 11 AU: Evidence for a continuously emitting "point" source, Ap. J. (Letters), 215, L89, 1977.

Scarf, F. L., Possible traversals of Jupiter's distant magnetic tail by Voyager and by Saturn, J. Geophys. Res., 84, 4422, 1979.

Scarf, F. L., W. S. Kurth, D. A. Gurnett, H. S. Bridge and J. D. Sullivan, Jupiter tail phenomena upstream from Saturn, Nature, 292, 585, 1981.

Scarf, F. L., D. A. Gurnett, W. S. Gurnett, and R. L. Poynter, Voyager-2 plasma wave observations at Saturn, Science, 215, 587, 1982.

Scarf, F. L., D. A. Gurnett, W. S. Kurth, and R. L. Poynter, Voyager plasma wave measurements at Saturn, J. Geophys. Res., this issue, 1983.

Schardt, A. W., F. B. McDonald, and J. H. Trainor, Energetic particles in the predawn magnetotail of Jupiter, J. Geophys. Res., 86, 8413, 1981.

Sckopke, N. and G. Paschman, The plasma mantle. A survey of magnetotail boundary layer observations, J. Atmos. Terr. Phys., 40, 261, 1978.

Siscoe, G. L., L. Davis, Jr., P. J. Coleman, Jr., E. J. Smith, D. E. Jones, Power spectra and discontinuities of the interplanetary magnetic field: Mariner 4, J. Geophys. Res., 73, 61, 1968.

Siscoe, G. L., N. F. Ness, and C. M. Yeates, Substorms on Mercury? J. Geophys. Res., 80, 4359, 1975.

Sonnerup, B. U. O. and L. J. Cahill, Magnetopause structure and attitude from Explorer 12 observations, J. Geophys. Res., 72, 171, 1967.

Thomas, B. T., and E. J. Smith, The structure and dynamics of the heliospheric current sheet, J. Geophys. Res., 86, 11105, 1981.

Villante, U., An overview by Pioneers observations of the distant geomagnetic tail, Space Sci. Rev., 20, 123, 1977.

TABLE 1

1981 Tail Events

Event no. Code*	Reference Code+	Duration Start-Stop (Day/Hour)		Identified by Experiment**
1	9	13/21	15/21	1, 2
	10	16/15	21/07	1, 2
2	12	48/12	55/20	1, 3
3	14	66/08	78/20	1, 2
4	15, 16, 17	92/00	103/09	1, 2
	18	106/18	108/21	1, 2
P	19	118/14	119/09	1, 4
5	21	140/21	148/20	1, 2
6	22	166/00	175/13	1, 4
		183/23	185/12	1
7	25	195/03	202/14	1, 4
8	26	227/06	228/06	1

* Event number Code refers to this work.

\+ Reference Code refers to code given in Table 1 of Kurth et al. (1982b) having an approximate correspondence.

** Key 1 = PLS
2 = PWS and PRA
3 = PRA
4 = PWS

TABLE 2

1981 CONTROL REGIONS

Duration Start-Stop (Day/Hour)		Notes
3/6	12/0	
26/0	34/18	
56/0	65/18	except all of day 61
80/0	88/18	
109/6	117/0	except all of day 115
128/6	137/0	
155/0	163/18	
175/18	183/18	
206/0	214/18	

TABLE 3

1981, V2 MAG EVENTS, i.e., $|\beta| \geq 60^\circ$

Event Number+	Start Day/Hr	---	Stop Day/Hr	Δt (Hours)	ΣΔt (Hours)
	1/5	---	1/15	10	
	2/22	---	3/0	2	
	18/0	---	18/2	2	
1	20/7	---	20/9	2	
	23/7	---	23/9	2	6
	48/5	---	48/14	9	
	49/23	---	50/1	2	
2	50/15	---	51/14	23	
	53/0	---	54/1	25	
	54/16	---	55/17	25	84
	61/7		f.b.p.*	≤1	
	67/13	---	67/20	7	
	69/4		f.b.p.	≤1	
3	72/10	s.b.v.**	74/9	47	
	76/14		f.b.p.	≤1	
	77/2	---	77/8	6	62
	77/21	---	77/23	2	
	78/11	---	78/14	3	
	90/0	---	f.b.p.	≤1	
	93/7	---	93/12	5	
	99/4	---	99/12	8	
	100/19	---	101/10	15	
4	102/1	---	102/23	22	
	105/3	---	105/6	3	
	106/22	---	107/1	3	
	108/7	---	108/11	4	60
	112/20	---	f.b.p.	≤1	
	114/6	---	114/15	9	
	115/13	---	115/15	2	
P	117/20	s.b.v.	119/6	34	45
	126/22		f.b.p.	≤1	
5	140/21	---	142/8	35	
	143/13	---	143/23	10	45
	145/5		f.b.p.	≤1	
	152/23		f.b.p.	≤1	
	157/21		f.b.p.	≤1	
	172/10	---	172/17	7	
6	174/23	---	175/11	12	
	184/5	---	185/16	35	54
	190/6	---	190/8	2	
	194/20		f.b.p.	≤1	
	201/0	---	201/2	2	
7	201/17	s.b.v.	202/0	7	
	202/13	---	202/15	2	11
	203/10		f.b.p.	≤1	
	205/17	---	205/19	2	
	209/8		f.b.p.	≤1	
	216/2	---	216/4	2	
	222/17	---	222/22	5	
8	223/11		f.b.p.	≤1	
	223/20	---	223/23	3	9

+Event number associated with Fig. 2
*f.b.p. = for a brief period
**s.b.v. = some brief violations

Figure Captions

Figure 1. The Voyager 2 trajectory in cylindrical coordinates (top sketch) and in Jupiter orbital plane coordinates (bottom sketch) in units of Jupiter radii (R_J = 71,398 km) for the period covered in Figure 2, which also defines times denoted 1 through 8 plus K and P. C.A. refers to the closest approach point to the Sun-Jupiter line. The spacecraft encountered Saturn about one week after event 8.

Figure 2. A survey of Voyager 2 Planetary Radio Astronomy (PRA), Plasma Science (PLS), Magnetometer (MAG), and Plasma Wave Science (PWS) data over a 287-day period. The top panel shows 2-hour averages amplitudes of PRA continuum radiation centered at 1.2 kHz, below which TAIL and CORE events are labeled 1 through 8 plus K and P (see text and Kurth et al., 1982b). The next panel gives daily averages of the PLS proton density. The bottom two panels show histograms giving the percent of hours in a day for which α satisfies the inequalities shown in the panels, where α is defined by the sketch in Figure 3. C.A. refers to the closest approach point to the Sun-Jupiter line.

Figure 3. A sketch giving the definitions of the angles α and β. The angle α is a cone angle measured with respect to the Jupiter direction, whereas β is a latitude angle measured with respect to a plane normal to the Jupiter-Spacecraft (S/C) line.

Figure 4. For the same period covered by Figure 2 the Voyager 2 PLS proton plasma speed (V) and number density (N) as well as the magnetic field magnitude (B) are shown, below which the 'TAIL' regions of Figure 2 are again given for reference. The bottom panel gives the percent of estimates in a day for which $\alpha_{\hat{n}} > 65°$, where $\alpha_{\hat{n}}$ is the angle between the Jupiter direction and an estimated minimum variance normal direction ($\hat{n}$) as computed from a variance analysis (see text).

Figure 5. Percent distributions of minimum variance normals based on Voyager 2 hour averages for the period shown in terms of heliographic longitude ($\lambda_{\hat{n}}$) and latitude ($\delta_{\hat{n}}$), in the top panels, and in terms of the cone angle $\alpha_{\hat{n}}$ defined in the caption of Figure 4, in the bottom panel. E_1, E_2, and E_3 are the maximum, intermediate and minimum eigenvalues, respectively, from the associated variance analyses. In the heliographic coordinate system angles are measured with respect to the $\hat{R}$-$\hat{T}$ plane at the spacecraft, where $\hat{R}$ is radially away from the sun and $\hat{T}$ is perpendicular to $\hat{R}$ and to the sun's spin axis; the longitude λ is measured counterclockwise from $\hat{R}$ in the $\hat{R}$-$\hat{T}$ plane as viewed from the north, and the latitude δ is positive northward and negative southward of the $\hat{R}$-$\hat{T}$ plane.

Figure 6. Percent distributions of minimum variance normals based on Voyager 1 hour averages for the period shown and given in the same format as that of Figure 5.

Figure 7. A survey of Voyager 1 magnetic field data for the first 150 days of 1981. The MAG panel is defined in the same way as that in Figure 2 and the $\hat{n}$-panel is described by the caption for Figure 4.

Figure 8. Percent histograms showing distributions of the magnetic field, in terms of its magnitude (B) and its heliographic longitude (λ) and latitude (δ), as well as the related Pythageroan mean RMS, denoted SIG. All quantities are based on hour average 'points' and the SIG's were derived from 48-s averages. The categories TAIL, CONTROL, and CORE refer to those shown in Figure 2 and defined in Tables 1 and 2, and in Kurth et al. (1982b) respectively, and were taken from 1981 data only.

Figure 9. Results of Voyager 2 correlation analyses using data from days 0-230, 1981. The top two panels give the correlation coefficient vs day-lag from a magnetic field autocorrelation analyses of $|\beta|$ for various conditions. The bottom panel gives the correlation coefficient vs day lag from MAG $|\beta|$-PRA wave amplitude cross correlation analyses for $|\beta| > 45°$. Recall that $\beta = 90° - \alpha$.

Figure 10. Event 5 in terms of (starting with the bottom panel): the magnetic field magnitude (B) and latitude cone-angle β, (solid curve); PLS plasma number density N, speed V, and derived ram pressure $m_p NV^2$; and PRA continuum wave amplitudes at 1.2 kHz. The dotted curve β_n in the β-panel represents minimum variance normal cone angles; see text. All quantities are based on hour averages. TAIL and CORE are from Table 1 and Kurth et al. (1982b), respectively.

Figure 11. A sketch of the expected "sausage-string" shape of the large-scale Jovian tail boundary resulting from periodic (25-day) solar wind pressure variations (Burlaga, 1983b). P refers to total external pressure.

Figure 12. Upper portion: A stylized sketch of the Jupiter orbital plane view of the distant Jovian magnetotail to the orbit of Saturn shown in relation to Voyager 2 encounters. The sketch conveys the likely possibility of filamentary structure. Where 'P' refers to total external pressure, the model shows qualitative but plausible width dimensions when the tail is in a low P region near Saturn, i.e., in a high P region near Jupiter (shaded area), and when it is a low P region at Jupiter (dashed curve). 'MP' refers to the magnetopause boundary. Lower portion: cross-sectional views of the tail for the two situations. The oval shape is due to the probable contribution of anisotropic $\vec{B}$ pressure to P (see text).

VOYAGER 2 TRAJECTORY

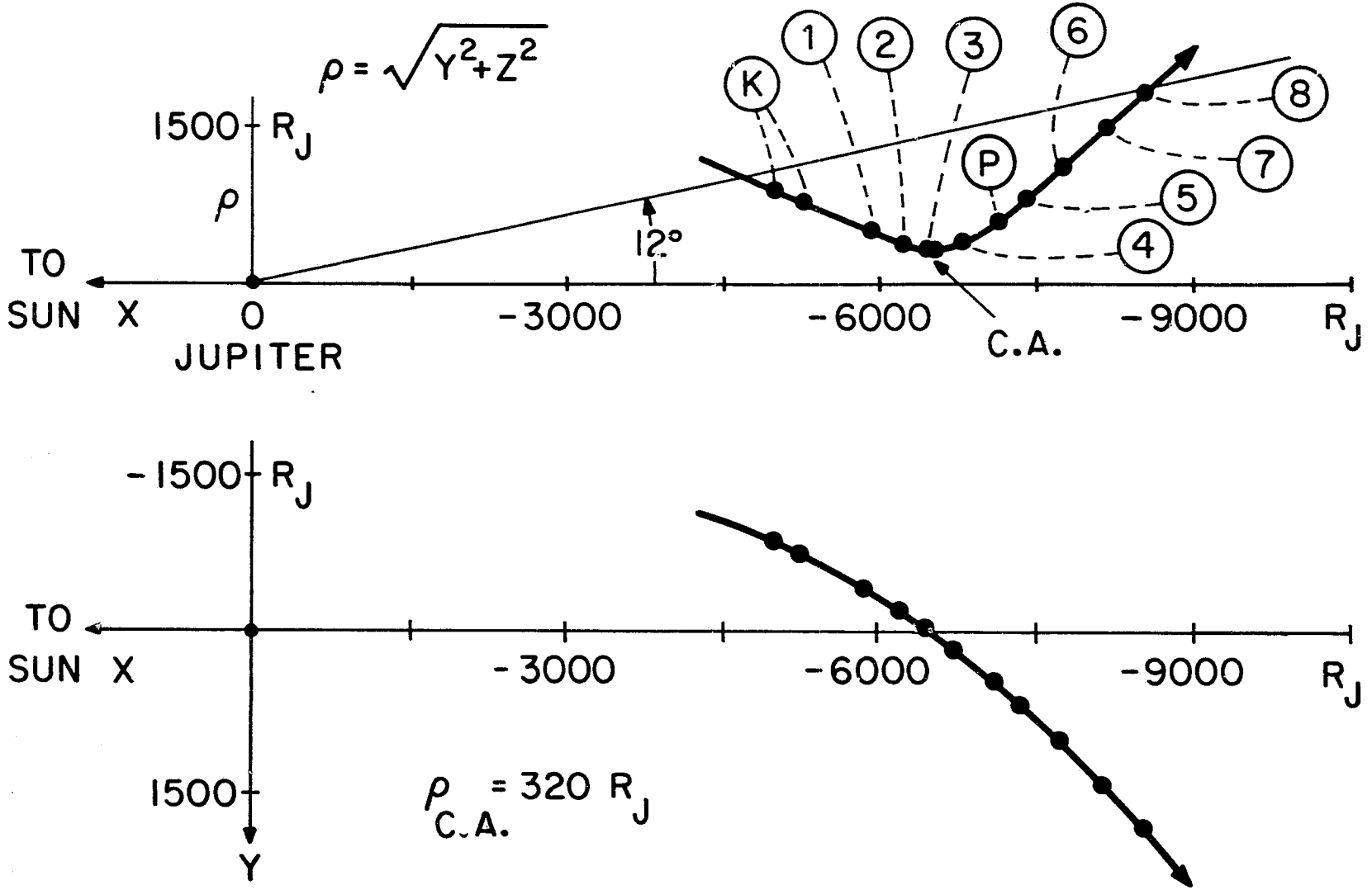

FIGURE 1

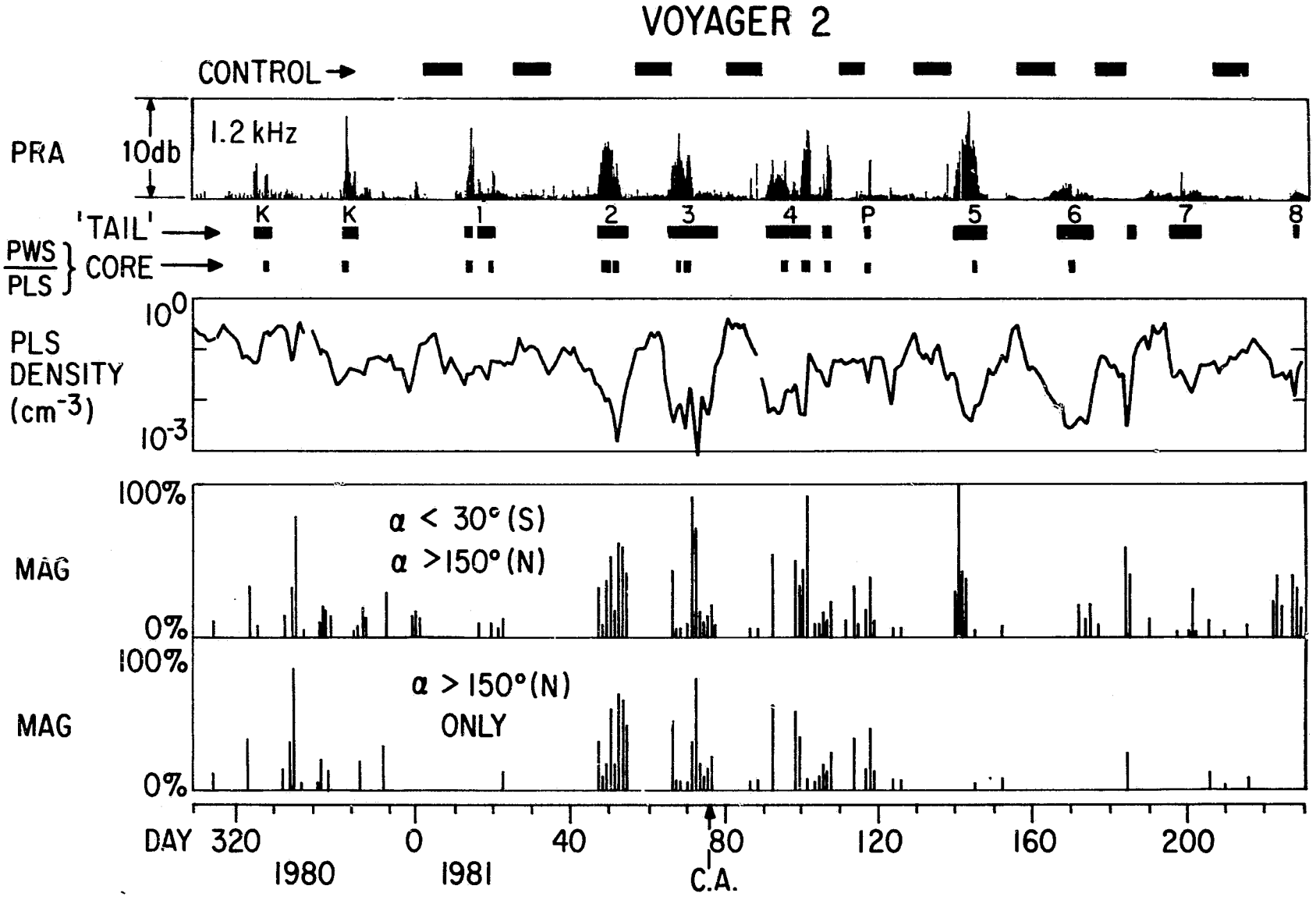

FIGURE 2

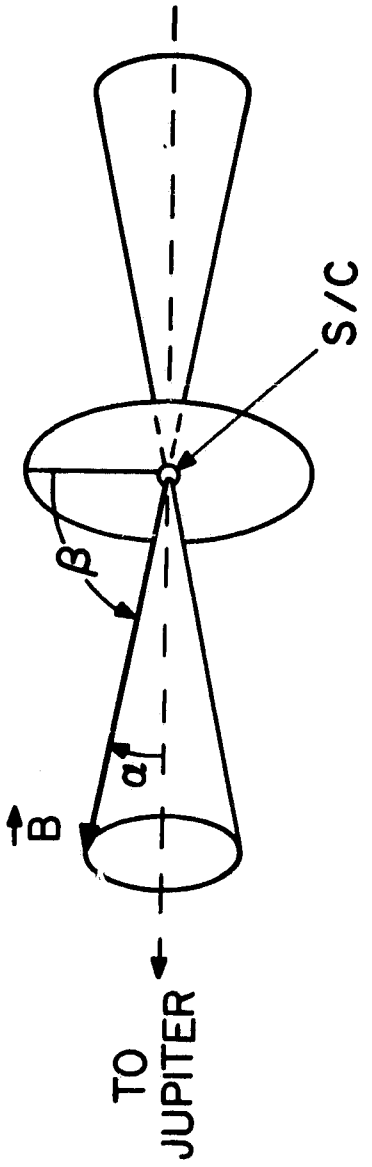

$\beta = 90° - \alpha$

FIGURE 3

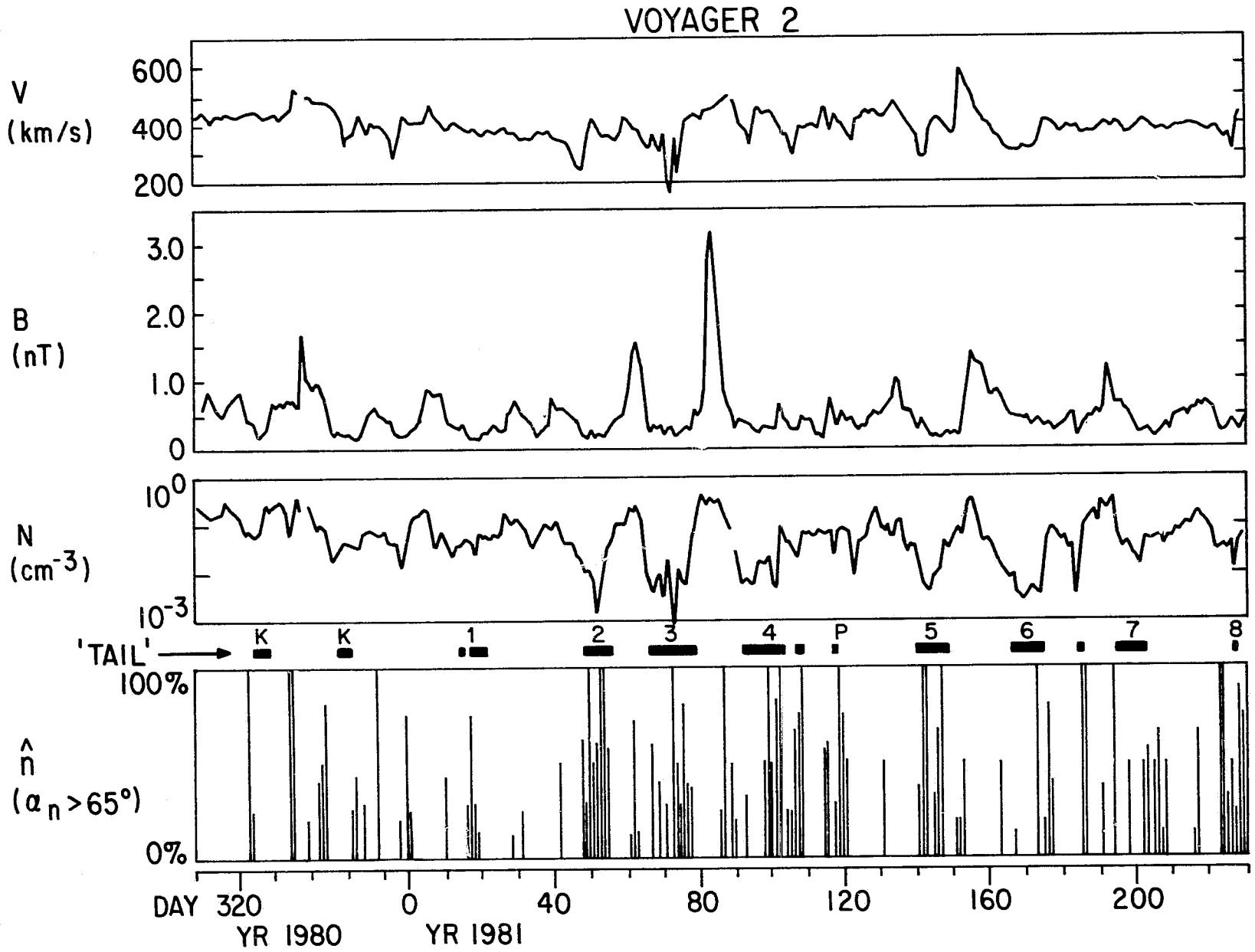

FIGURE 4

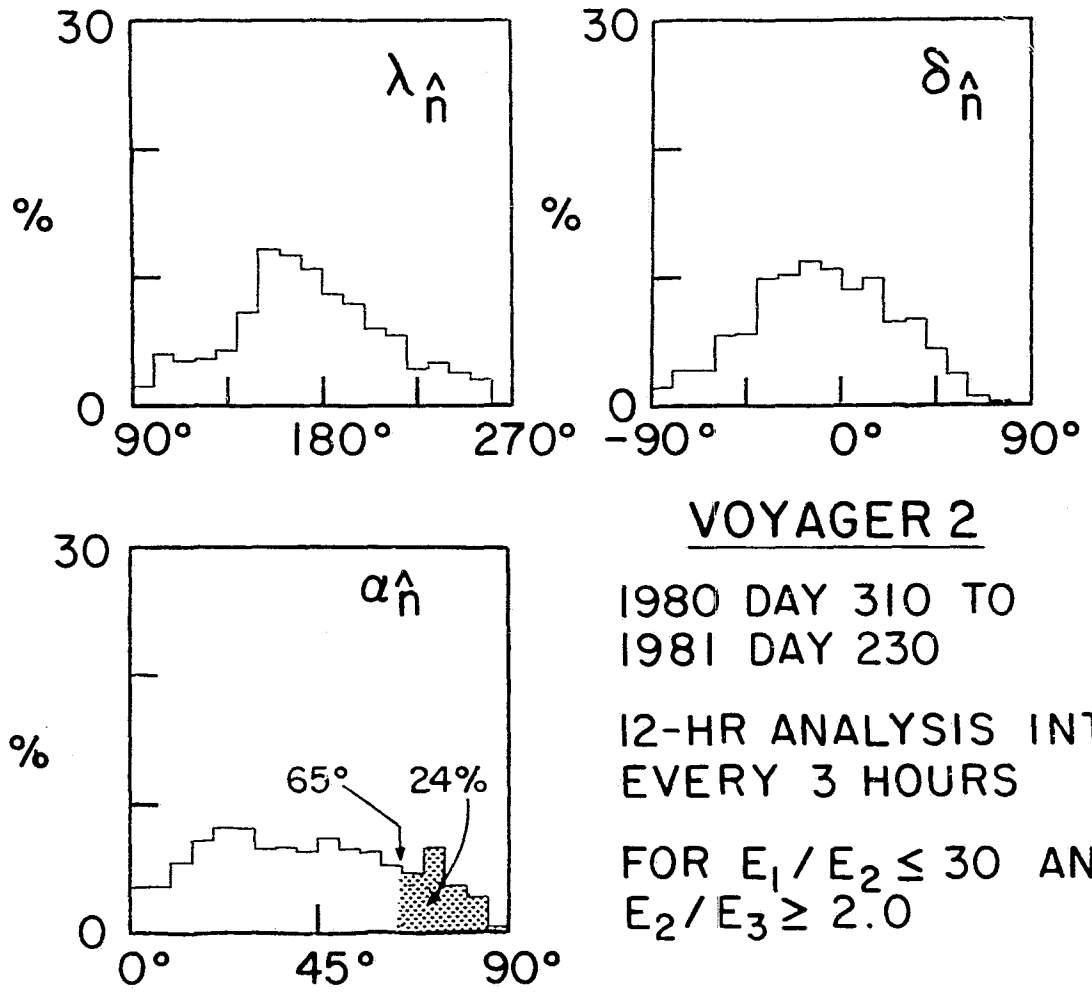

VOYAGER 2

1980 DAY 310 TO
1981 DAY 230

12-HR ANALYSIS INTERVALS
EVERY 3 HOURS

FOR $E_1 / E_2 \leq 30$ AND
$E_2 / E_3 \geq 2.0$

FIGURE 5

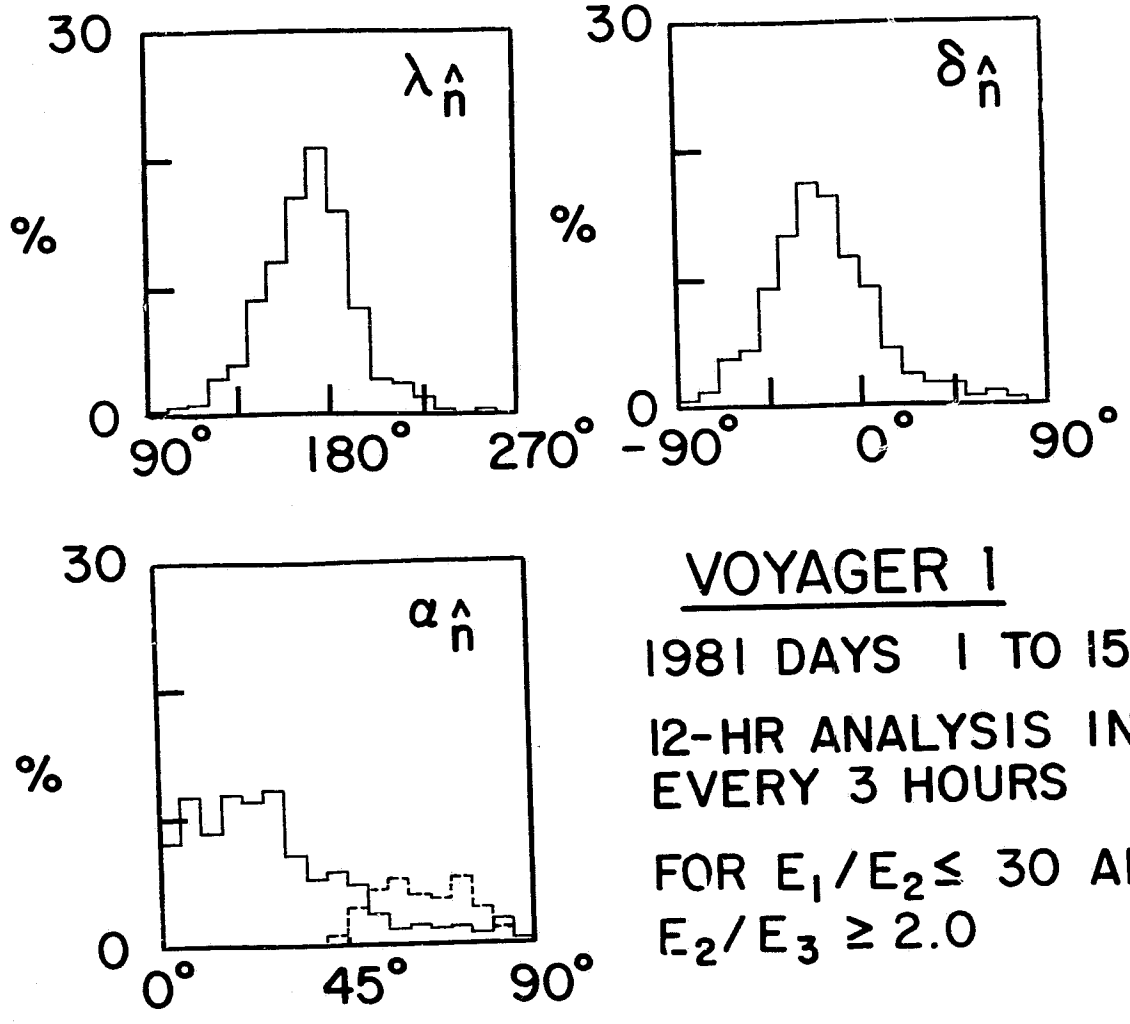

FIGURE 6

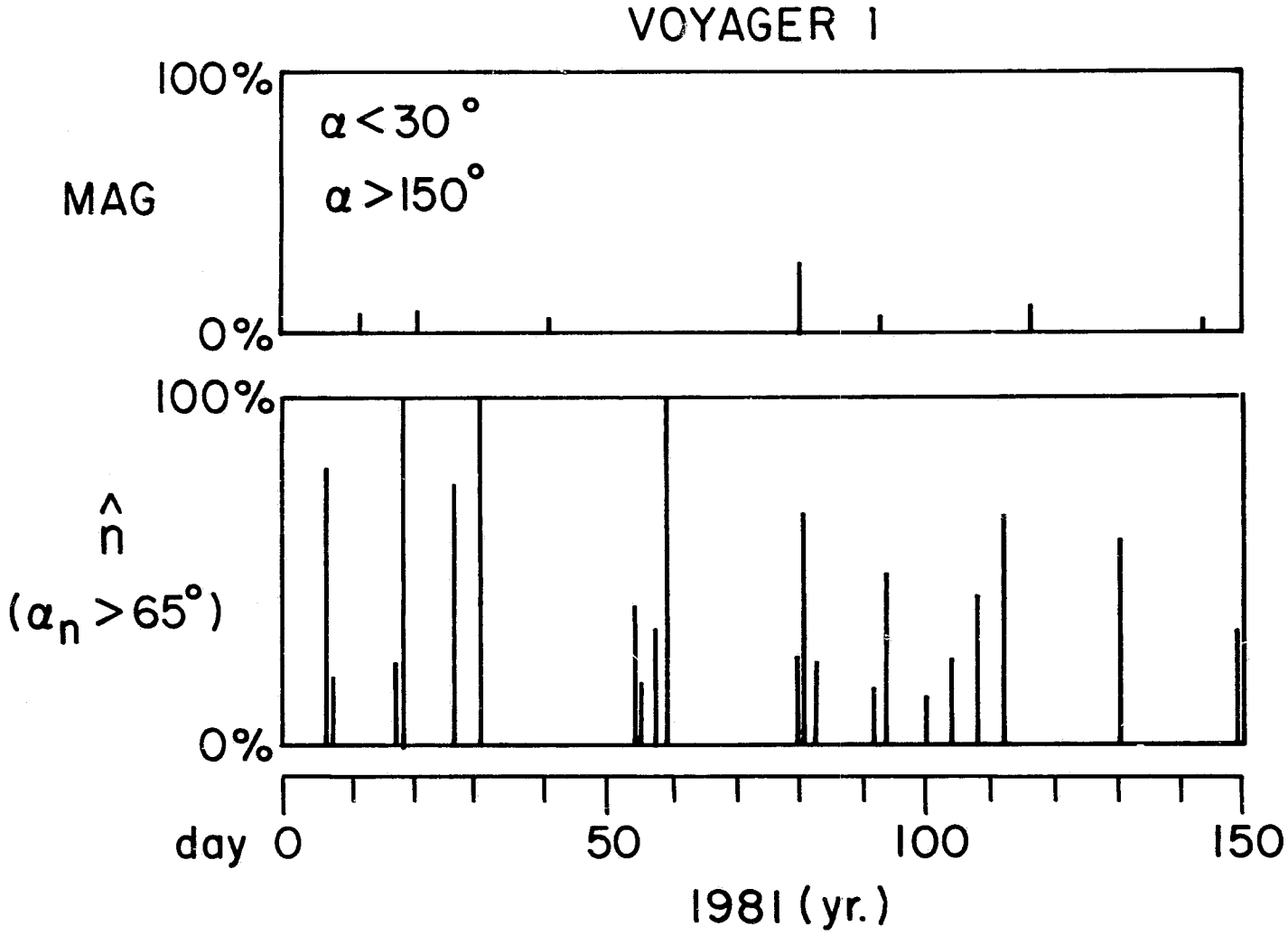

FIGURE 7

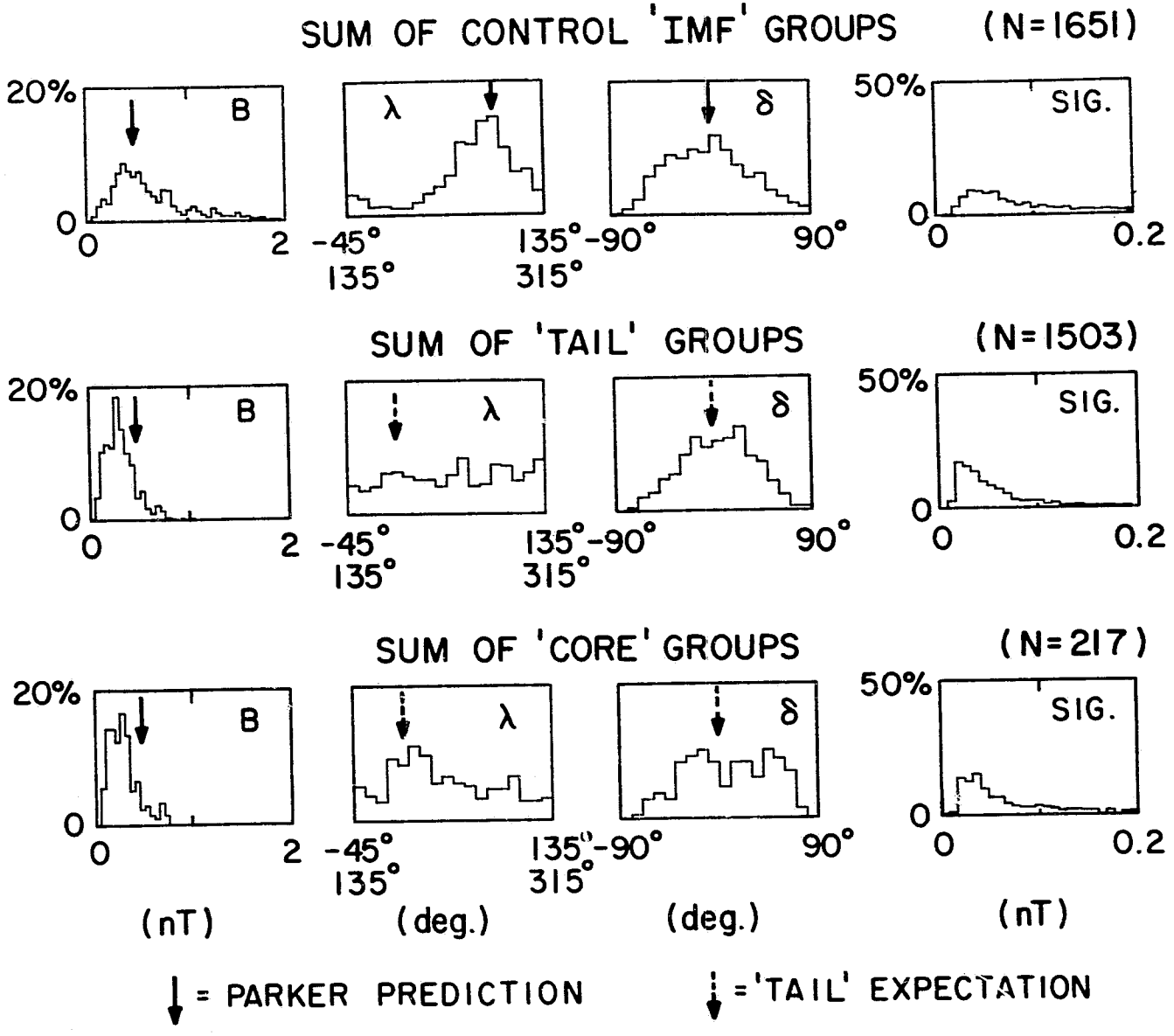

FIGURE 8

VOYAGER 2

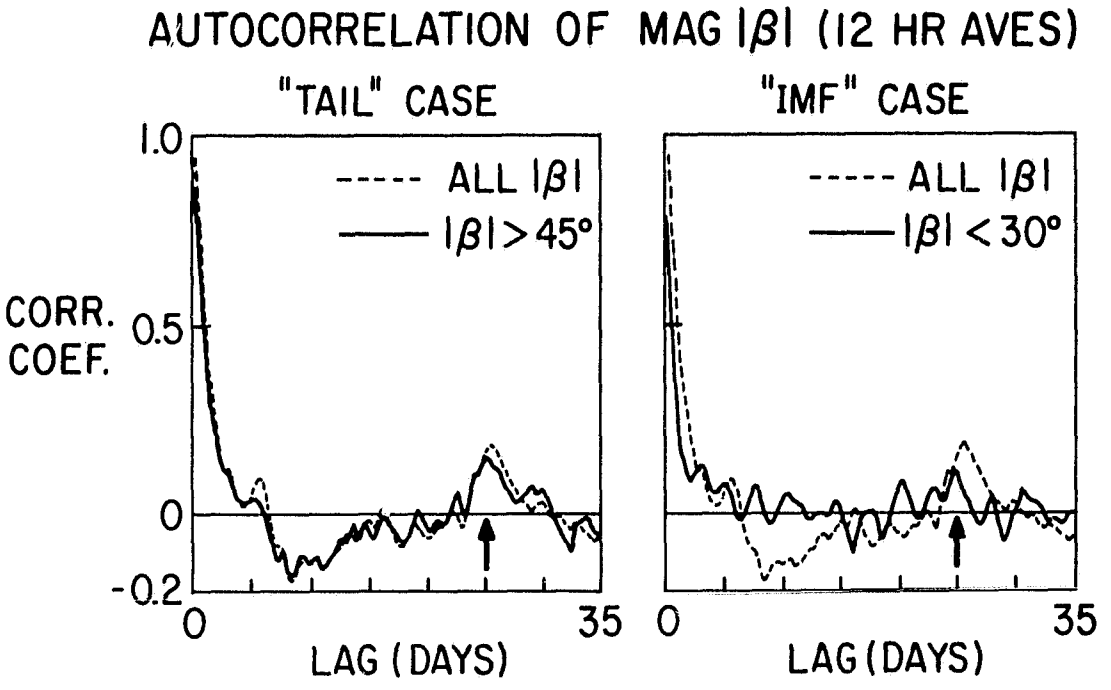

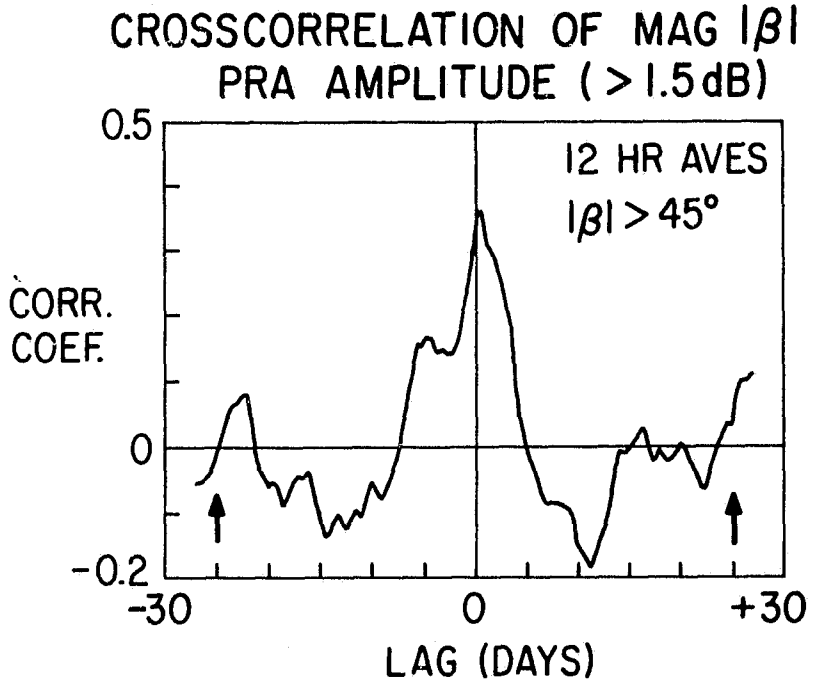

FIGURE 9

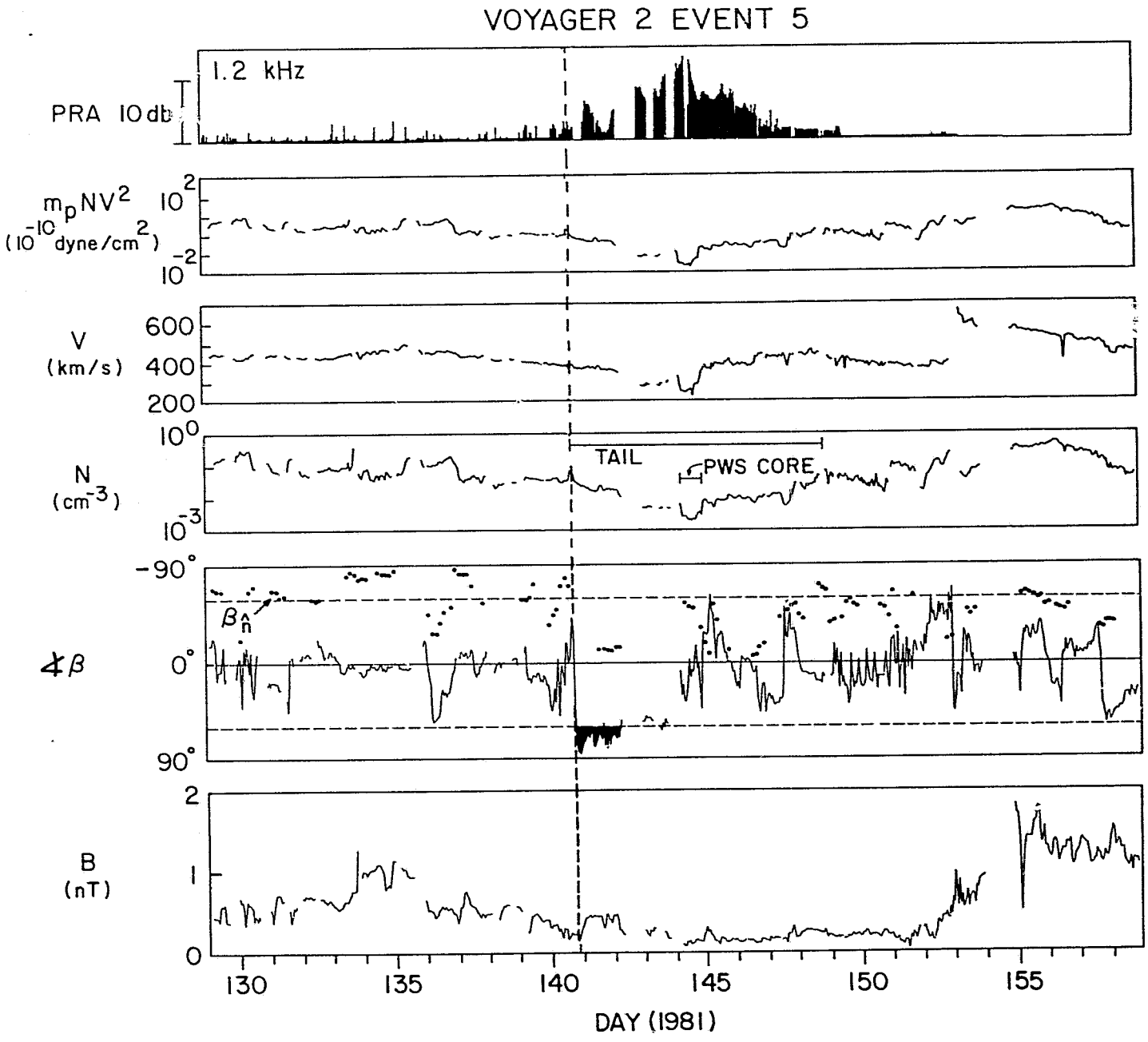

FIGURE 10

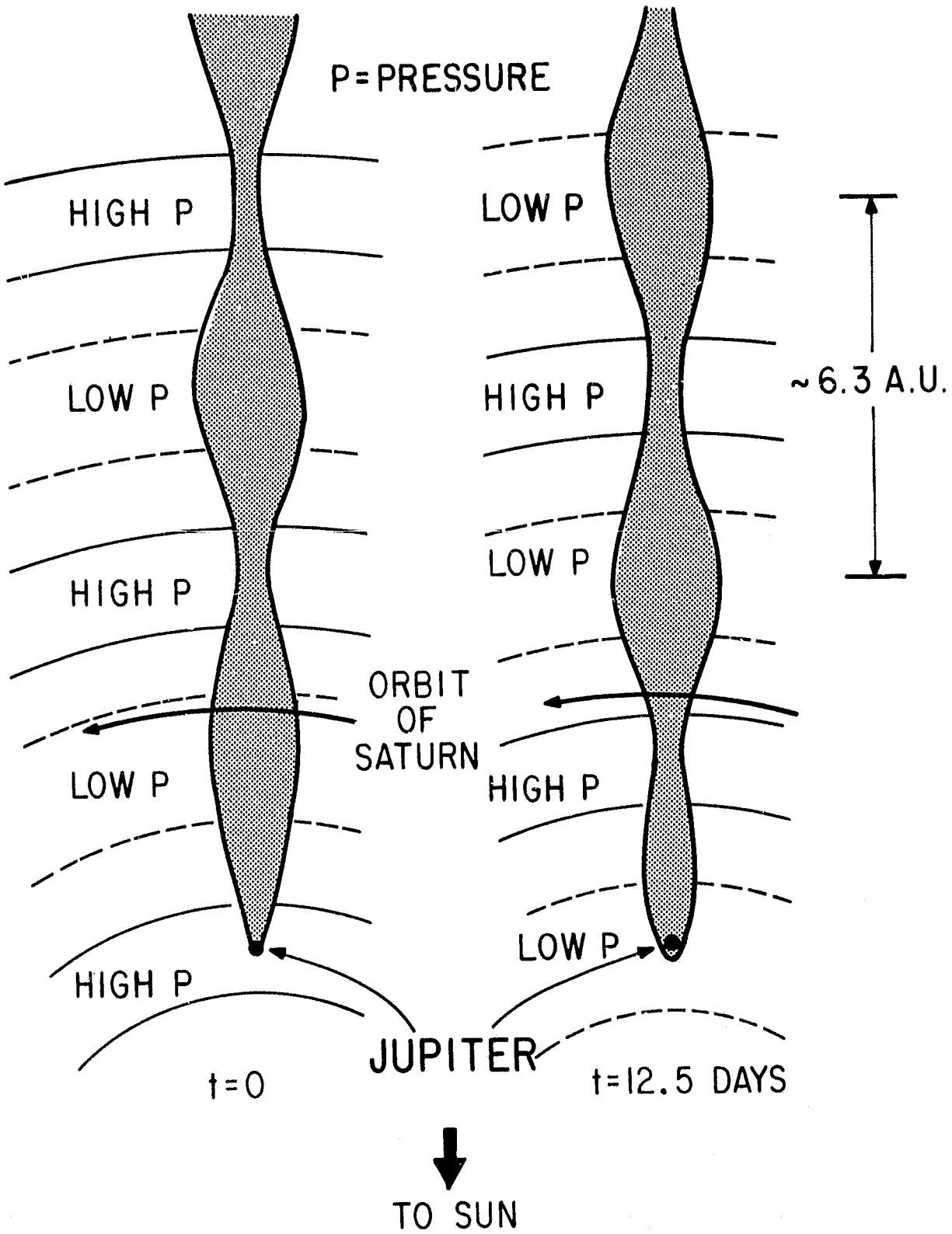

FIGURE 11

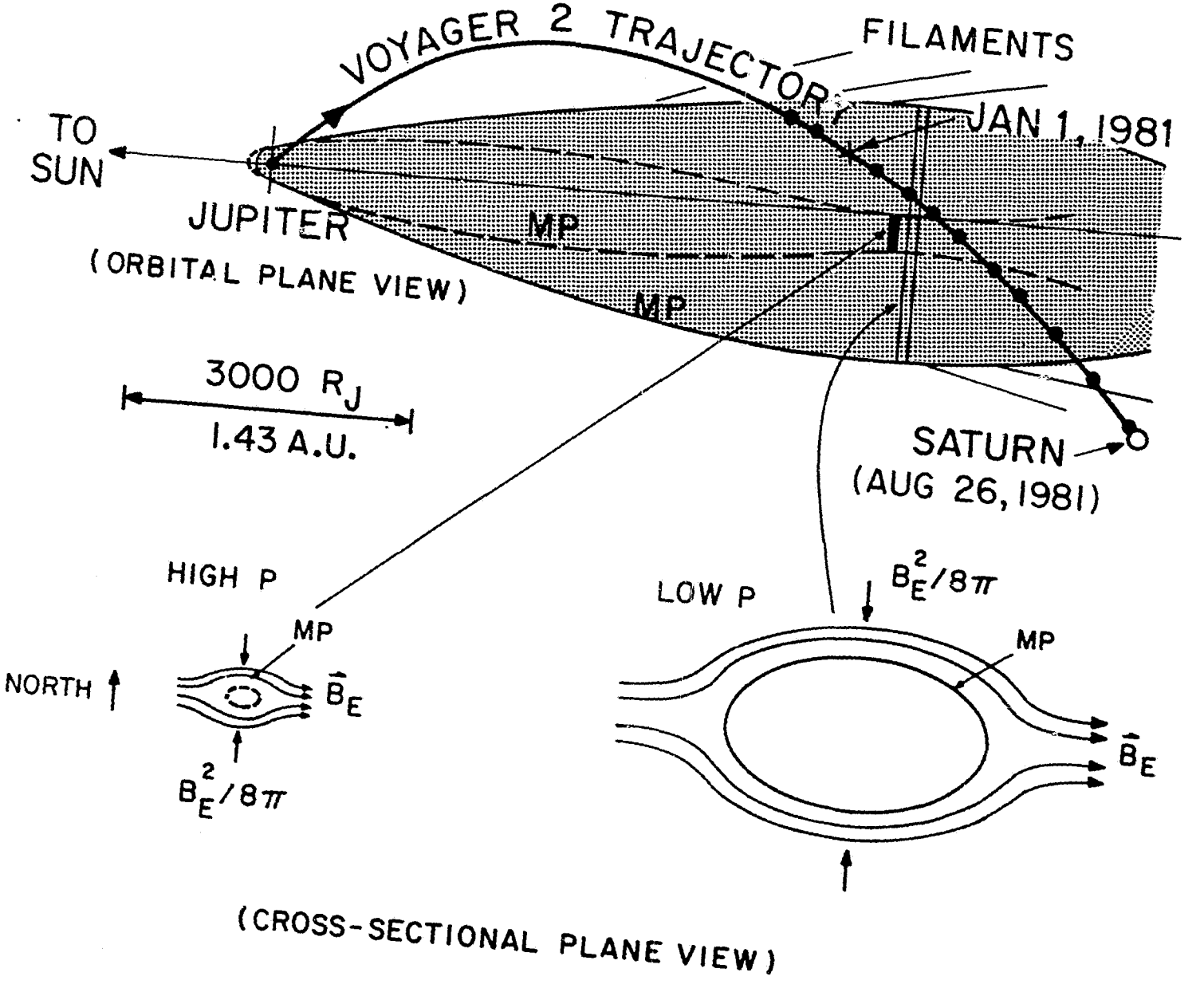

FIGURE 12